Localization and screening anomalies in two-dimensional systems

A. Gold
Physik-Department der Technischen Universität München, D-8046 Garching bei München, Germany

W. Götze
Physik-Department der Technischen Universität München, D-8046 Garching bei München, Germany and Max-Planck-Institut für Physik und Astrophysik, D-8000 München 40, Germany

(Received 9 January 1985)

The self-consistent current theory for two-dimensional electron dynamics in strongly disordered environments is extended by an approximative incorporation of Coulomb interaction effects. Quantitative details of the theory are worked out for a Si(100) metal-oxide-semiconductor device at zero temperature which is doped with Na ions. The results are compared with experiments on the nonlinear variation of the resistivity with impurity concentration, on the mobility suppression for low electron concentration, on the metal-insulator phase-transition diagram, on the nonmonotonic variation of the dynamical conductivity with electron concentration, and with the results of laser-light absorption. Predictions are made about impurity-induced plasmon shifts and dampings, and on a depletion-field-induced mobility suppression which may lead to a metal-insulator transition. A long-time anomaly for current relaxations is predicted to yield a singular non-Drudian current spectrum showing up as a conductivity peak at very low frequencies.

I. INTRODUCTION

In this paper some features of two-dimensional electron dynamics caused by disorder will be discussed. As an application, we have in mind the Si(100) metal-insulator-semiconductor device, doped with Na^+ ions. The qualitative discussion holds for other systems as well. We will restrict ourselves to low-temperature situations so that a zero-temperature theory is adequate.

There is a large body of experimental and theoretical work concerning the Si(100) metal-oxide-semiconductor (MOS) system, which is reviewed in a recent article by Ando, Fowler, and Stern.[1] For the above-mentioned system, the electron density n can be varied over several orders of magnitude. Hence, that device provides an example for a many-particle system, where the transition from weak to strong coupling can be studied experimentally. Surface imperfections always provide some disorder for the electron motion and this is one cause for a finite particle mobility and for plasmon damping. The disorder will also lead to electron localization in Anderson's[2] sense. Therefore, the MOS system offers for study the disorder-induced conductor-insulator transition, as was pointed out by Mott.[3] This holds even more so, since by drifting Na^+ ions to the interface, one has a means to vary disorder in a controllable fashion.[4,5] Many disorder-induced effects have been reported which cannot be understood within the established kinetic-equation approach (KEA) towards the electron dynamics. Besides the existence of a mobility edge, originally detected by the transition from activated to metallic conductivity due to a change of n,[6] let us mention the following: a nonlinear increase of the current relaxation rate with the impurity density n_i,[5] a strong suppression of the mobility below the KEA result at low density n,[4] pronounced deviations of the current spectra from the Drude Lorentzians,[7] and a nonmonotonic variation of the dynamical conductivity with electron density.[8]

In order to treat the electron dynamics beyond the KEA, the self-consistent current-relaxation theory shall be developed. This approach, whose essence is a self-consistent treatment of current relaxation and density propagation, was proposed originally for the motion of noninteracting electrons in random potentials; in particular, the evaluation of conductivities near the Anderson transition was intended.[9–11] This theory was applied for a schematic model of two-dimensional electron systems in order to analyze some experiments for Si-MOS systems.[12–14] In the present paper previous work will be extended to deal with charged impurities and to take the electron-electron interaction into account. In this way a self-consistent treatment of localization, dynamical screening phenomena, and plasmon dynamics will be achieved.

It was discovered that quantum interference effects cause characteristic anomalies in the dynamics of two-dimensional systems of noninteracting electrons.[15] For example, there is a logarithmic increase of the resistivity, of some percentage per decade, of decreasing temperature, which was observed also for high-mobility Si-MOS devices.[16] The relevance of the interference effects for strongly disordered MOS devices is not understood at present and we are going to ignore them completely. It is known how quantum interference effects can be incorporated into the present theory, such that the correct asymptotic laws are obtained.[17] In this paper we focus exclusively on effects which are not related to singularities possibly influenced by interference effects. In this case, it is not known how the treatment of the backscattering anomalies[15] can be incorporated into our approximation scheme without running into the problem of double

counting. Neither is it known how to incorporate inelastic phonon processes into the formalism, and so only such experiments, where the experimentalists either have carried out the extrapolation to zero temperature or where the temperature variations can be absorbed into the experimental error bars, will be analyzed. We will also ignore the logarithmic interaction corrections present in weakly disordered systems.[18] Because of a lack of evidence to the contrary, we adopt the view that the mentioned effects are so small that they do not show up on the scales to be used for our discussion of theoretical and experimental results.

The paper will be structured as follows. To make the work self-contained, we report in Sec. II those specifications of the model and definitions of correlation functions which will enter the calculations. In Sec. III the approximation scheme is developed. Self-consistency equations are derived which yield as a solution the current and density correlation functions. The equations extend our previous work by using a realistic model for the electron layer and for the random potential due to ion scatterers. The singular Coulomb-interaction effects between the electrons are incorporated within the random-phase approximation modified by a Hubbard approximation for local-field corrections. In Sec. IV the results are shown in detail. First, it is demonstrated (Sec. IV A) that the lowest-order approximation of the present theory for the mobility μ_0 extends the previous theory[19] by incorporation of local-field corrections in the screening function. In Sec. IV B mobility suppression as the precursor of localization is explained. The theory yields a conductor-insulator transition due to disorder (Sec. IV C) which can be viewed as an Anderson transition in a random potential modified by screening. The anomalous polarization effects in two-dimensional systems imply an $n_i \propto n^{4/3}$ law for the critical impurity density for small electron densities. The superposition of ion scattering and surface roughness scattering and the suppression of the mobility for high electron densities is demonstrated in Sec. IV D. A depletion-field-induced metal-insulator transition is discussed in Sec. IV E. Strong deviations of the relaxation spectrum from a white-noise spectrum, discussed in Sec. IV F, imply a strong deviation of the dynamical conductivity $\sigma(\omega)$ versus the frequency ω curve from the Drude Lorentzian. The anomalies can be viewed as plasma-wave-emission contributions to the conductivity. The plasmons get a damping because of the electron impurity scattering. The scattering rate depends on the screening which in turn is ruled by the plasmon dynamics. In Sec. IV G the corresponding results for the plasmon damping and shifts are calculated, for long-wavelength plasmons become overdamped due to disorder. As a result, there appears an anomalous diffusion mode whose excitation leads to a characteristic long-time tail anomaly for the conductivity, which is calculated in Sec. IV H. Finally, (Sec. IV I) a series of current spectra is presented in order to show the change of the electron dynamics, from the one typical for an almost free-electron gas, to one characteristic of a Fermi glass. A conclusion is given in Sec. V. We demonstrate that the theory to be exposed can give a unified physical interpretation of an almost quantitative explanation of a series of disorder testing experiments done for Si(100) MOS systems.

II. THE MODEL

In this section the concepts to be used will be listed. The free-electron eigenstates for the motion parallel to the surface are $\psi_{\mathbf{k}}(\mathbf{r},x)=\psi(x)\exp(i\mathbf{k}\cdot\mathbf{r})$. Here, and in the following, $\mathbf{k},\mathbf{p},\mathbf{q}$ labels two-dimensional wave vectors, $\mathbf{r}$ denotes two-dimensional position vectors, and x denotes the spacial direction perpendicular to the surface. A unit area of the surface will be considered. $a^*_{\mathbf{k}\alpha}$ and $a_{\mathbf{k}\alpha}$ denote fermion creation and annihilation operators for the mentioned states. The degeneracy index $\alpha=1,2,\ldots,2g_v$ is introduced to label the two spin states and the g_v valleys in which the electron can be. An isotropic parabolic band is assumed so that the electron energies are characterized by the effective mass m: $\varepsilon_{\mathbf{k}}=k^2/2m$; units are chosen such that $\hbar=1$. The density of states then is a constant $\rho_F=g_v m/\pi$ so that the Fermi energy $\varepsilon_F=k_F^2/2m$ and the electron density n are related linearly: $n=\rho_F\varepsilon_F$; k_F denotes the Fermi momentum. The free-fermion-gas Hamiltonian then reads $H_0=\sum_{\mathbf{k},\alpha}\varepsilon_{\mathbf{k}}a^*_{\mathbf{k}\alpha}a_{\mathbf{k}\alpha}$ and for this system all correlation functions can be calculated explicitly. The dynamical susceptibility $\chi(\mathbf{q},z)$ for the density fluctuations of wave vector $\mathbf{q}$,

$$\rho(\mathbf{q})=\sum_{\mathbf{k},\alpha} a^*_{\mathbf{k}-\mathbf{q}/2,\alpha}a_{\mathbf{k}+\mathbf{q}/2,\alpha}\ ,$$

reads[20]

$$\chi_0(\mathbf{q},z)=(\rho_F/2Q^2)\{2Q^2+[Z-Q(Q-1)]^{1/2}[Z-Q(Q+1)]^{1/2}-[Z+Q(Q-1)]^{1/2}[Z+Q(Q+1)]^{1/2}\}\ . \tag{1a}$$

Here, and in the following, z denotes the complex frequency off the real axis and $Z=z/4\varepsilon_F$, $Q=q/2k_F$. In particular, we will need the wave-vector-dependent compressibility $g(\mathbf{q})=\chi(\mathbf{q},z=i0)$:

$$g_0(\mathbf{q})=\rho_F[1-\Theta(Q^2-1)(Q^2-1)^{1/2}/Q]\ . \tag{1b}$$

Due to their charge e, the fermions will experience a Coulomb interaction which can be described by the Hamiltonian

$$H_c=\tfrac{1}{2}\sum_{\mathbf{q}}\rho^+(\mathbf{q})v(q)\rho(\mathbf{q})\ ,$$

where

$$v(q)=(2\pi e^2/\bar{\epsilon}q)F(q)\ . \tag{2a}$$

Here, $\bar{\epsilon}=\frac{1}{2}(\epsilon_1+\epsilon_2)$ is the average dielectric constant of the two media separated by the surface of electron motion. $F(q)$ is a form factor which can be expressed in terms of ϵ_1, ϵ_2, and $\psi(x)$ (Ref. 19) (see also Ref. 1, Eq. 2.51). If $q/b\ll 1$, where $1/b$ is a characteristic thickness parameter, one gets $F(q)\cong 1$. For $q/b\gg 1$ the form factor tends to zero. In this paper no contribution to the theory of electron-electron interaction is intended. Rath-

er, we assume the system parameters to be chosen, such that the random-phase approximation, complemented by Hubbard's approximation for local-field corrections[21]

$$G(q)=q/[2g_v(q^2+k_F^2)^{1/2}] ,$$

is an appropriate treatment (see, e.g., Pines and Nozières[22] for a discussion). The dynamical density susceptibility for the interacting system then reads

$$\chi_c(\mathbf{q},z)=\chi_0(\mathbf{q},z)/[1+v_{\rm eff}(q)\chi_0(\mathbf{q},z)] , \tag{2b}$$

where the effective potential is given by $v_{\rm eff}(q)=v(q)[1-G(q)]$. Since both $G(q)$ and $F(q)-1$ vanish for $q\to 0$, the long-wavelength compressibility tends to zero proportional to q, with a slope given in terms of ρ_F and the Thomas-Fermi screening vector $q_s=2\pi e^2\rho_F/\bar{\epsilon}$ (Ref. 20)

$$g_c(\mathbf{q})=g_0(\mathbf{q})/[1+v_{\rm eff}(q)g_0(\mathbf{q})]$$
$$=\rho_F(q/q_s)+O(q^2) . \tag{2c}$$

The excitation spectrum described by Eq. (2b) consists of two contributions. First, there is a continuous spectrum due to particle-hole excitations:

$$\chi_c''(\mathbf{q},\omega)=\chi_0''(\mathbf{q},\omega)/|1+v_{\rm eff}(q)\chi_0(\mathbf{q},\omega+i0)|^2 ,$$
$$\chi_0''(\mathbf{q},\omega+i0)\neq 0 . \tag{2d}$$

Here, and in the following, correlation functions $F(z)$ near the real frequency axis are written as $F(\omega\pm i0)=F'(\omega)\pm iF''(\omega)$. Let us mention also that the spectral function $F''(\omega)$ determines the general correlation function in terms of a spectral integral:

$$F(z)=\int d\omega F''(\omega)/[\pi(\omega-z)] .$$

Second, for wave vectors $q<q^*$, where q^* is of the order $2k_F$, the denominator in Eq. (2b) vanishes for some real frequency $\omega_p(q)$. This implies a sharp resonance in $\chi_c''(\mathbf{q},\omega)$ situated above the particle-hole continuum: the well-known plasma resonance.[22] For $qv_F\ll|z|$, Eq. (1a) yields the expansion $\chi_0(\mathbf{q},z)\cong -nq^2/(mz^2)$, and thus the small-$q$ plasmon dispersion law is readily found as[23,24]

$$\omega_p(q)^2=[2\pi e^2n/(m\bar{\epsilon})]q+O(q^2) . \tag{2e}$$

The deviations of the plasma dispersion from the asymptotic $\omega_p\propto\sqrt{q}$ law are influenced by the form factor $F(q)$ and the local-field corrections $G(q)$.[21] It is an important feature of the two-dimensional electron dynamics, as opposed to the three-dimensional one, that the long-wavelength plasma frequency tends to zero.

We want to study the influence of disorder on the electron dynamics. The disorder shall be characterized by a random potential, whose Fourier transform will be denoted by $U(\mathbf{q})$. The random-potential average is absorbed in the system's chemical potential, so that $\langle U(\mathbf{q})\rangle_{\rm dis}=0$. The electron-disorder-interaction Hamiltonian reads

$$H'=\sum_{\mathbf{q}} U(\mathbf{q})\rho^*(\mathbf{q}) . \tag{3a}$$

The random potential we assume to consist of two uncorrelated parts: $U_i(\mathbf{q})$, due to ions drifted to the electrons, and $U_d(\mathbf{q})$, due to defects such as, e.g., surface roughness. So one writes

$$\langle|U(\mathbf{q})|^2\rangle_{\rm dis}=\langle|U_i(\mathbf{q})|^2\rangle_{\rm dis}+\langle|U_d(\mathbf{q})|^2\rangle_{\rm dis} . \tag{3b}$$

If the ions with charge e_i are distributed with density n_i and static structure factor

$$s(q)=\left\langle\sum_{ab}\exp[i\mathbf{q}(\mathbf{r}_a-\mathbf{r}_b)]\right\rangle_{\rm dis}\Big/n_i ,$$

where $\mathbf{r}_a,\mathbf{r}_b$ are the ion positives, one gets

$$\langle|U_i(\mathbf{q})|^2\rangle_{\rm dis}=n_i[2\pi ee_i/(\bar{\epsilon}q)]^2s(q)|F_i(q)|^2 . \tag{3c}$$

Here again $F_i(\mathbf{q})$ is a form factor expressible in terms of ϵ_1, ϵ_2, $\psi(x)$, and the distance z_i between the ion layer and the electron layer.[19] Actually, $F_i(q)$ should also contain the effects of lattice distortions created by the ions. Again one gets $F_i(q\to 0)=1$ and $F_i(q\to\infty)=0$. The defect potential shall be parametrized by a strength factor U and a spatial extension parameter $L_0=2\pi/q_0$:

$$\langle|U_d(\mathbf{q})|^2\rangle_{\rm dis}=4\pi U^2\Theta(q_0-q)/q_0^2 . \tag{3d}$$

For quantitative discussions we will restrict ourselves to the Si(100) MOS system, since this device has been studied extensively before. In this case, $\epsilon_1=11.5$, $\epsilon_2=3.9$, so that $\bar{\epsilon}=7.7$ and m equal 0.19 electron masses; $g_v=2$. As ions, we consider Na^+, so that $e_i=-e$. Since, unfortunately, nothing is known about short-range-order effects of the ion layer, we assume complete randomness $s(q)=1$. We are interested in anomalies connected with plasmon excitations and localization in Coulomb fields. To study these effects one often uses the mathematical model of a truly two-dimensional system without additional disorder: $F=F_i=1$, $U_d=0$. This model is specified by the only two experimental parameters n and n_i. If one wants to compare the results for this model with experiment, one has to use n_i as a fit parameter. The fitted n_i should be smaller than the experimental value since the form factors will effectively weaken the interaction effects. One should also either eliminate the effects of defect scattering, caused, for example, by surface roughness, from the data, or use the model only under such circumstances where ion scattering dominates over defect scattering.

To analyze the results for a more realistic model, the simplified form factors, as they follow from the variational function

$$\psi(x)^2=(b^3/2)x^2\exp(-bx)$$

of Ref. 25, shall be used. For the sake of completeness let us quote the results[19] explicitly. The one entering $v_{\rm eff}(q)$ reads (see also Ref. 1, Eqs. 2.52, 3.30, and 3.31)

$$F(q)=\left\{\tfrac{1}{16}(\epsilon_1+\epsilon_2)\left[8+9\frac{q}{b}+3\left[\frac{q}{b}\right]^2\right]+\tfrac{1}{2}(\epsilon_1-\epsilon_2)\Big/\left[1+\frac{q}{b}\right]^3\right\}\Big/\left[\epsilon_1\left[1+\frac{q}{b}\right]^3\right] . \tag{4a}$$

The parameter for the inverse thickness is given by $b^3=48\pi m_\perp e^2 n^*/\epsilon_1$, where the mass for perpendicular motion $m_\perp$ is 0.916 times the electron mass and n^* is composed of electron density and depletion-layer density $n_{\rm depl}$: $n^*=N_{\rm depl}+\frac{11}{32}n$. The form factor entering $U_i(\mathbf{q})$ reads

$$F_i(q)=1\Big/\left[\exp(qz_i)\left[1+\frac{q}{b}\right]^3\right] . \tag{4b}$$

So this more realistic model is specified by the one additional parameter $N_{\rm depl}$. If the surface roughness is the origin of defect scattering, one can follow Ando[26] and write

$$U=\gamma\Delta , \tag{5}$$

where γ depends on $N_{\rm depl}$ and n according to $\gamma=(4\pi e^2/\bar{\epsilon})(N_{\rm depl}+\frac{1}{2}n)$. Δ is a length parameter of the order of some angstroms independent of n and $N_{\rm depl}$ and so is L_0 (which corresponds to $\pi\Lambda$ in Ref. 1, Eqs. 4.56 and 4.57).

The dynamical properties to be calculated shall be phrased in terms of Kubo functions or propagators[27]: $\Phi_{AB}(z)=(A\mid(\mathcal{L}-z)^{-1}\mid B)$. The Liouvillian is defined by $\mathcal{L}A=[H,A]$ and the scalar product is given by disorder-averaged thermodynamic compressibilities at zero temperature:

$$(A\mid B)=\left\langle\int_0^\beta d\lambda\langle[\langle A^*B(i\lambda)\rangle-\langle A^*\rangle\langle B\rangle]\rangle\right\rangle_{\rm dis} , \qquad \beta\to\infty .$$

The spectral function of $\Phi(z)$ is trivially related to the one for the impurity-averaged susceptibility if $\omega\neq 0$; $\Phi''_{AB}(\omega)=\langle\langle\langle A^*;B\rangle\rangle''_\omega\rangle_{\rm dis}/\omega$. If the A or B are ergodic variables, one can prove $\Phi_{AB}(z)=[\langle\langle A^*;B\rangle\rangle_z-(A\mid B)]/z$. However, if A and B exhibit nonergodic motion, the Kubo function has a characteristic zero-frequency pole $z\Phi_{AB}(z)\to -f$, $z\to 0$. The residue f quantifies the difference between the thermodynamic susceptibility and the static limit of the dynamical susceptibility: $\langle\langle A^*;B\rangle\rangle_{z=i0}+f=(A\mid B)$.

The density propagator $\Phi(q,z)$, i.e., the Kubo function formed with $A=B=\rho(\mathbf{q})$, will be used to study the shift and broadening of plasmon excitations in the system due to disorder. The propagator for the undisturbed system, $\Phi_c(\mathbf{q},z)$, will enter the following calculation [it is given by the susceptibilities defined in Eqs. (2b) and (2c)]:

$$\Phi_c(\mathbf{q},z)=[\chi_c(\mathbf{q},z)-g_c(\mathbf{q})]/z . \tag{6}$$

Applying the reduction formalism of Zwanzig[28] and Mori,[29] one can write for the propagator

$$\Phi(\mathbf{q},z)=-g(\mathbf{q})/[z+q^2K(\mathbf{q},z)/g(\mathbf{q})] .$$

Here, $g(\mathbf{q})=(\rho(\mathbf{q})\mid\rho(\mathbf{q}))$ is the static density compressibility of the system. The continuity equation $\mathcal{L}\rho(\mathbf{q})=-qj(\mathbf{q})$ was used, which connects density changes with the longitudinal current density $j(\mathbf{q})$. Then

$$K(\mathbf{q},z)=(j(\mathbf{q})\mid(Q\mathcal{L}Q-z)^{-1}\mid j(\mathbf{q}))$$

with

$$QA=A-\rho(\rho\mid A)/g(\mathbf{q}) .$$

In the long-wavelength limit, $K(\mathbf{q}\to 0,z)=K(z)$ is the velocity correlation function. Its absorptive part denotes, up to a factor e^2, the dynamical conductivity[27]

$$\sigma(\omega)=e^2K''(\omega) . \tag{7}$$

Of particular interest will be the dc conductivity $\sigma=\sigma(\omega=0)$ or, equivalently, the mobility $\mu=\sigma/(ne)$.

Applying the Zwanzig-Mori reduction on the velocity correlation function, one arrives at the representation[30]

$$K(z)=-(n/m)/[z+M(z)] . \tag{8a}$$

Here the identity $(j\mid j)=\langle\langle\mid j(\mathbf{q}),\rho(\mathbf{q})\mid\rangle\rangle_{\rm dis}=n/m$, expressing the f-sum rule, was used. The kernel $M(z)$ is the correlation function of the fluctuating forces $F(t)=F(t,q\to 0)$,

$$F(\mathbf{q},t)=\exp(i\mathcal{L}'t)\mathcal{L}j(\mathbf{q}) ;$$

$\mathcal{L}'=Q'\mathcal{L}Q'$ with Q' projecting perpendicular to $j(\mathbf{q})$:

$$M(z)=(\pm im/n)\int dt\,\Theta(\pm t)\exp(izt)(F(t)\mid F(t=0)) , \qquad \mathrm{Im}z\gtrless 0 . \tag{8b}$$

If there is no disorder, the particle momentum is conserved: $\mathcal{L}j=0$; in this case, $M(z)=0$. Hence, a nonzero $M(z)$ is caused by disorder and it describes the relaxation towards zero of induced currents due to momentum transfer of impurities and defects to the electron system. If $M(z)=\pm i/\tau$ for $\mathrm{Im}z\gtrless 0$, Eq. (8a) is the Drude formula. Hence, the absorptive part of the current relaxation kernel $M(z)$, the current relaxation spetrum $M''(\omega)$, generalizes Drude's current relaxation rate $1/\tau$ to a frequency-dependent function. If the relaxation spectrum varies with frequency, causality requires the reactive part $M'(\omega)$ to be nonzero. Let us note also, that the zero-frequency relaxation spectrum is, up to a trivial factor, identical with the inverse mobility

$$1/\mu=(m/e)M''(\omega=0) . \tag{8c}$$

III. SELF-CONSISTENT CURRENT RELAXATION THEORY

In this section the approximation scheme, to be used for an evaluation of the current relaxation kernel $M(z)$ and the density propagator $\Phi(q,z)$, shall be formulated. The fluctuating force is found to consist of products of random-potential gradients and density fluctuations

$$F(\mathbf{q})=\sum_{\mathbf{k}}(\mathbf{q}-\mathbf{k})U(\mathbf{q}-\mathbf{k})\rho(\mathbf{k})/m .$$

A lowest-order factorization approximation will be applied in Eq. (8b): averages of products of U and ρ are approximated by products of averages of random-potential fluctuations and on averages of density fluctuations[9,10]

$$M(z)=\sum_{\mathbf{q}}\langle\mid\mathbf{q}U(\mathbf{q})\mid^2\rangle\Phi(\mathbf{q},z)/nm . \tag{9}$$

This formula can be rephrased in several ways. According to the golden rule, the decay rate $M''(\omega)$ of the momentum is given by the square of the relevant coupling

matrix element $\mathbf{q}U(\mathbf{q})$ times the density of states $\Phi''(q,\omega)$ for the decay process. The q sum over all decay processes has to be carried out and the spectral representation for $M(z)$ and $\Phi(q,z)$ transfers the formula

$$M''(\omega)=\sum_{\mathbf{q}}\langle\,|\,\mathbf{q}U(\mathbf{q})\,|^2\rangle\Phi''(\mathbf{q},\omega)/nm$$

into the corresponding one for the z-dependent quantities. Equation (9) can also be viewed as a simplified version of a mode coupling approximation, originally introduced by Kawasaki[31] in a different context. The current mode j is not conserved because it can decay into other modes of the system. The simplest decay modes in our system are pair modes consisting of density fluctuations with momentum $\mathbf{q},\rho(\mathbf{q})$ and random-potential fluctuations of momentum $-\mathbf{q},U(\mathbf{q})^*$. The latter may be viewed as static phonons. Formula (9) can also be viewed as an analogue of the self-consistent Born approximation studied usually for the electron propagators.[32] It shares the virtue of this approximation in not being a weak coupling approach. It also shares the defects of that approach by not being able to handle impurity bands. The binding of electrons at the impurities, a phenomenon which one expects to occur for $n_i\to 0$ and $U\to 0$ for our model, cannot be treated by a simple factorization procedure. Therefore, we have to assume disorder to be such that impurity bands are absent or that the Fermi energy is so far above the impurity bands that the latter can be ignored. The precise range of validity of Eq. (9) is unknown at present. In formula (9), interaction effects and screening phenomena are hidden in $\Phi(q,z)$ (Ref. 33), as will be seen in Sec. IV A.

To discuss approximations for the density propagator, we want to consider all correlation functions formed with the phase-space densities

$$f_{\mathbf{k}}(\mathbf{q})=\sum_{\alpha}a^*_{\mathbf{k}-\mathbf{q}/2,\alpha}a_{\mathbf{k}+\mathbf{q}/2,\alpha}\ .$$

The corresponding correlation functions and susceptibilities will be denoted by

$$\Phi_{\mathbf{kp}}(\mathbf{q},z)=(f_{\mathbf{k}}(\mathbf{q})\,|\,(\mathscr{L}-z)^{-1}\,|\,f_{\mathbf{p}}(\mathbf{q}))$$

and

$$g_{\mathbf{kp}}(\mathbf{q})=(f_{\mathbf{k}}(\mathbf{q})\,|\,f_{\mathbf{p}}(\mathbf{q}))\ .$$

It is convenient to orthonormalize the variables by introducing $A_n(\mathbf{q})=\sum_{\mathbf{k}}a^n_{\mathbf{k}}f_{\mathbf{k}}(\mathbf{q})$ such that $(A_n\,|\,A_m)=\delta_{nm}$. The general Mori equation for

$$\Phi_{nm}(\mathbf{q},z)=(A_n\,|\,(\mathscr{L}-z)^{-1}\,|\,A_m)$$

then reads (see Ref. 29 or the book by Forster[34] for details)

$$[z\delta_{nl}-\omega_{nl}(\mathbf{q})+m_{nl}(\mathbf{q},z)]\Phi_{lm}(\mathbf{q},z)=-\delta_{nm}\ . \tag{10a}$$

Here, $\omega_{nm}=(A_n\,|\,\mathscr{L}\,|\,A_m)=\langle\langle[A_n^*,A_m]\rangle\rangle_{\rm dis}$, the $m_{nl}(\mathbf{q},z)$ are the usual memory kernels, and the summation convention is used. If one defines a reference function $\Phi^R_{\rm ln}(\mathbf{q},z)$ as the solution of the equation

$$[z\delta_{nl}-\omega_{nl}(\mathbf{q})]\Phi^R_{lm}(\mathbf{q},z)=-\delta_{nm}\ , \tag{10b}$$

one can rewrite Eq. (10a) in the form of a matrix Dyson equation

$$\Phi_{nm}(\mathbf{q},z)=\Phi^R_{nm}(\mathbf{q},z)+\Phi^R_{ns}(\mathbf{q},z)m_{st}(\mathbf{q},z)\Phi_{tm}(\mathbf{q},z)\ . \tag{10c}$$

The density is the distinguished variable of our discussion and so let us choose $A_0=\rho(\mathbf{q})/\sqrt{g(\mathbf{q})}$, such that $\Phi_{00}(\mathbf{q},z)=\Phi(\mathbf{q},z)/g(\mathbf{q})$. The fundamental particle conservation law is reflected in the present approach by

$$\mathscr{L}\rho(\mathbf{q})=\sum_{\mathbf{k}}(\mathbf{k}\cdot\mathbf{q}/m)f_{\mathbf{k}}(\mathbf{q})\ ,$$

so that the fluctuating forces on A_0 vanish: $m_{0\alpha}=m_{\alpha 0}=0$. To get some understanding of the solution of Eqs. (10), the collision-rate approximation of the kinetic gas theory[35] will be imitated. We replace the matrix m_{st} by a diagonal one, but observe the mentioned conservation law:

$$m_{st}(\mathbf{q},z)=\delta_{st}(1-\delta_{s0})(1-\delta_{t0})m(\mathbf{q},z)\ .$$

We approximate further by ignoring the wave-vector dependence of the kernel: $m(\mathbf{q},z)=\tilde{M}(z)$. Then one finds

$$\Phi_{nm}(\mathbf{q},z)=\Phi^R_{nm}(\mathbf{q},\zeta)-\tilde{M}(z)[1+M(z)\Phi^R_{00}(\mathbf{q},\zeta)]^{-1}\times\Phi^R_{n0}(\mathbf{q},\zeta)\Phi^R_{0m}(\mathbf{q},\zeta)\ , \tag{11}$$

where $\zeta=z+\tilde{M}(z)$. So the phase-space correlation functions are expressed in terms of the one unknown kernel $\tilde{M}(z)$ and the reference functions $\Phi^R_{nm}(\mathbf{q},\zeta)$. To discuss the latter let us rewrite Eq. (10b) for the susceptibilities $\chi^R_{\mathbf{kp}}=z\Phi^R_{\mathbf{kp}}+g_{\mathbf{kp}}$ formed with the Wigner functions $f_{\mathbf{k}}(\mathbf{q})$:

$$z\chi^R_{\mathbf{kp}}(\mathbf{q},z)-\omega_{\mathbf{ks}}(g^{-1})_{st}\chi^R_{tp}(\mathbf{q},z)=-\omega_{\mathbf{kp}}\ . \tag{12a}$$

One finds also $\omega_{\mathbf{kp}}=\delta_{\mathbf{kp}}(n_{\mathbf{k}+\mathbf{q}/2}-n_{\mathbf{k}-\mathbf{q}/2})$ with the occupation numbers

$$n_{\mathbf{k}}=\sum_{\alpha}\langle\langle a^*_{\mathbf{k}\alpha}a_{\mathbf{k}\alpha}\rangle\rangle_{\rm dis}\ .$$

So the reference function is determined in a complicated manner in terms of $n_{\mathbf{k}}$ and $g_{\mathbf{kp}}(\mathbf{q})$; both set of functions are influenced by disorder as well as by electron-electron interactions. Within the random-phase approximation, interaction effects on $n_{\mathbf{k}}$ are ignored, except for rigid-band shifts. In the same spirit we shall ignore the effects of disorder and write $n_{\mathbf{k}}=\Theta(\varepsilon_F-\varepsilon_{\mathbf{k}})$. Similarly, the compressibilities shall be replaced by the random-phase-approximation result

$$g_{\mathbf{kp}}=\delta_{\mathbf{kp}}g^0_{\mathbf{k}}(\mathbf{q})-v_{\rm eff}(q)g^0_{\mathbf{k}}(\mathbf{q})g^0_{\mathbf{p}}(\mathbf{q})[1+g^0(\mathbf{q})v_{\rm eff}(q)]^{-1}\ ,$$

where

$$g^0_{\mathbf{k}}(\mathbf{q})=(n_{\mathbf{k}-\mathbf{q}/2}-n_{\mathbf{k}+\mathbf{q}/2})/(\mathbf{q}\cdot\mathbf{k}/m)\ .$$

Hence, Eq. (12a) reduces to

$$(z+\mathbf{q}\cdot\mathbf{k}/m)\chi^R_{\mathbf{kp}}(\mathbf{q},z)-(n_{\mathbf{k}+\mathbf{q}/2}-n_{\mathbf{k}-\mathbf{q}/2})v_{\rm eff}(q)\sum_{\mathbf{e}}\chi_{\mathbf{ep}}(\mathbf{q},z)=-(n_{\mathbf{k}+\mathbf{q}/2}-n_{\mathbf{k}-\mathbf{q}/2})\delta_{\mathbf{kp}}\ . \tag{12b}$$

This separable integral equations is the random-phase approximation for the phase-space susceptibilities[36] and so our reference functions are approximated by the random-phase approximation for the interacting system, mentioned in connection with Eqs. (2). In particular, the density propagator is derived from Eq. (11) as

$$\Phi(\mathbf{q},z)=\frac{\Phi^c[\mathbf{q},z+\tilde{M}(z)]}{\{1+\tilde{M}(z)\Phi^c[\mathbf{q},z+\tilde{M}(z)]/g^c(\mathbf{q})\}} . \tag{13}$$

Quite a few approximations were used to derive this explicit expression of $\Phi(\mathbf{q},z)$ in terms of the not yet specified kernel $\tilde{M}(z)$. The derivation was done with the motivation of carrying out in each step the simplest meaningful approximation. At present, no means are known by which one may judge the range of validity of the approach. But it is again evident that anomalies in the density of states are ignored. Neither impurity band effects nor band tail effects can be studied. Equation (13) differs from the one used originally for a noninteracting electron gas[9-11] in the sense that Φ^c and g^c are not free-gas functions, but rather the functions of the system with interaction.

Let us consider the normalized longitudinal current $A_1=j(\mathbf{q})/\sqrt{nm}$. For the reference functions, one verifies by an explicit check

$$\Phi_{01}(\mathbf{q},z)=\frac{1}{q}[g(\mathbf{q})+z\Phi(\mathbf{q},z)]/[g(\mathbf{q})n/m]^{1/2} , \tag{14a}$$

$$\Phi_{11}(\mathbf{q},z)=\frac{z}{q^2}[g(\mathbf{q})+z\Phi(\mathbf{q},z)](m/n) . \tag{14b}$$

These formulas express the known fact that the random-phase approximation preserves the exact relations between longitudinal currents and density derivatives. Using these properties, one verifies that also the solutions of Eq. (11) obey Eqs. (14). Thus, the truncation of the matrix m_{st} by the one-kernel matrix preserves the exact relations between Φ_{00}, Φ_{01}, and Φ_{11} also. From Eqs. (1a), (2b), and (6), one derives the expansion

$$g_c(\mathbf{q})/\Phi_c(\mathbf{q},\zeta)=-\zeta[\,1-\{nq^2/[mg_c(\mathbf{q})\zeta^2]\}+O((qv_F/\zeta)^4)] .$$

Substitution of this result into Eq. (13) yields the Green-Kubo formula of the present theory: up to terms of order $O(qv_F/\zeta)^2q^2K(z)/g(\mathbf{q})$ in the denominator of $\Phi(\mathbf{q},z)$, one gets

$$\Phi(\mathbf{q},z)=-g_c(\mathbf{q})/[z+q^2K(z)/g_c(\mathbf{q})] . \tag{15a}$$

Here, $K(z)=-(n/m)/\zeta$. Substitution of this result into Eq. (14b) leads to the long-wavelength expansion for the longitudinal current correlation function

$$\Phi_L(\mathbf{q},z)=(j(\mathbf{q})\,|\,(\mathscr{L}-z)^{-1}\,|\,j(\mathbf{q}))=(n/m)\Phi_{11}(\mathbf{q},z) .$$

Thus, we have

$$\Phi_L(\mathbf{q},z)=zK(z)/[z+q^2K(z)/g_c(\mathbf{q})] . \tag{15b}$$

Since $q^2/g_c(\mathbf{q})$ vanishes in the long-wavelength limit, Eq. (2c), $K(z)=\Phi_L(\mathbf{q}=0,z)$. Thus, $K(z)$ is indeed the velocity correlation function introduced before in connection with Eq. (7). Comparing the present representation of $K(z)$ with the formula (8a), one identifies $\tilde{M}$ with the current-relaxation kernel M:

$$M(z)=\tilde{M}(z) . \tag{16}$$

Remembering from the preceding section that $\langle\,|\,U(\mathbf{q})\,|^2\rangle$ is given by our model of disorder and that the reference functions of the system without disorder, Φ_c and g_c, are given as well, one concludes that Eqs. (9), (13), and (16) are closed nonlinear equations in order to determine $M(z)$, $K(z)$, and $\Phi(\mathbf{q},z)$. These equations can be solved by iteration, as was done before for the case of noninteracting electrons.[11,12] In the following section the results will be discussed in detail. The approximation scheme formulates a self-consistency problem. The current-relaxation rate depends on the density excitation spectrum. Obviously, the transfer rate of recoil from the disorder to the electrons has to depend on the dynamical properties of the electron system. Equation (9) formulates this fact approximately. On the other hand, the current-relaxation rate rules the current propagation, Eq. (8a), and via the continuity equation the latter rules the density propagation. For long wavelength, this connection between $K(z)$ and $\Phi(\mathbf{q},z)$ is given by Eq. (15a), and for general q, the connection is formulated approximately by Eqs. (13) and (16). Current relaxations and density propagations have to be evaluated simultaneously.

Let us note some general properties of the approximation scheme. If $M(z)$ is analytic for $\mathrm{Im}z\neq 0$ and if it has a spectral representation with $M''(\omega)=M''(-\omega)\geqq 0$, the same holds for $K(z)$ in Eq. (8a) and $\Phi(\mathbf{q},z)$ in Eq. (13). The latter statement holds under the assumption that $\Phi_c(\mathbf{q},z)$ is a correlation function with the standard properties. Conversely, any $\Phi(\mathbf{q},z)$ which exhibits a spectral representation with a non-negative spectral function yields an $M(z)$ from Eq. (9) with the same properties. No matter how $M(z)$ is chosen otherwise, provided it is analytic for $\mathrm{Im}z\neq 0$ and $M(z)/z\to 0$ for $z\to\infty$, Eqs. (7) and (8a) yield the sum rule for the conductivity

$$\int d\omega\,\sigma(\omega)=\pi e^2n/m , \tag{17a}$$

and Eq. (13) yields the compressibility sum rule

$$\int d\omega\,\Phi''(\mathbf{q},\omega)=\pi g_c(\mathbf{q}) \tag{17b}$$

and the f-sum rule for the density spectrum

$$\int d\omega\,\omega^2\Phi''(\mathbf{q},\omega)=\pi(nq^2/m) . \tag{17c}$$

The Ward identities, i.e., the connections between $\Phi_{0\alpha}$ and $\Phi_{1\alpha}$ which follow from the continuity equation, are fulfilled also; Eqs. (14) are special cases.

The mode coupling equation (9), together with the sum rule (17b), leads to a sum rule for the current-relaxation spectrum

$$\int d\omega\,M''(\omega)=\pi\tilde{\omega}_1^2 , \tag{18a}$$

where

$$\tilde{\omega}_1^2=\sum_{\mathbf{q}}\langle\,|\,\mathbf{q}U(\mathbf{q})\,|^2\rangle g_c(q)/nm . \tag{18b}$$

On the other hand, the exact Mori representation (8b) yields on the right-hand side of Eq. (18a) the fre-

quency $\omega_1^2=(F\,|\,F)m/n$. One gets $(F\,|\,F)=(\mathscr{L}j\,|\,F)=\langle\langle[j^*,F]\rangle\rangle_{\rm dis}$, i.e.,

$$\omega_1^2=\sum_{\mathbf{q}} q^2\langle\langle U(\mathbf{q})^*\rho(\mathbf{q})\rangle\rangle_{\rm dis}/2nm \ . \tag{18c}$$

If it were possible to evaluate the characteristic frequency ω_1 for the disordered system, or to get a reliable approximation for it, the deviation between ω_1 and $\tilde{\omega}_1$ could be used as a means to quantify the error of Eq. (9).

IV. DISCUSSION

A. Nearly-free-electron-gas mobility

The lowest-order approximation for the current-relaxation spectra is obtained if in Eq. (9) the density spectrum of the Fermi liquid without disorder is substituted:

$$M_0''(\omega)=\sum_{\mathbf{q}} q^2\langle\,|\,U(\mathbf{q})\,|^2\rangle\Phi_c''(\mathbf{q},\omega)/2mn \ . \tag{19}$$

For the zero-frequency rate $1/\tau=M_0''(\omega=0)$, one finds with Eqs. (6) and (2d)

$$1/\tau=\sum_{\mathbf{q}} q^2\langle\,|\,U_{sc}(\mathbf{q})\,|^2\rangle\Phi_0''(\mathbf{q},\omega=0)/2mn \ , \tag{20a}$$

where

$$U_{sc}(\mathbf{q})=U(\mathbf{q})/[1+g_0(\mathbf{q})v_{\rm eff}(q)] \ . \tag{20b}$$

The free-gas zero-frequency density spectrum follows from Eqs. (1) and (6) to

$$\Phi_0''(q,\omega=0)=\rho_F(qv_F)^{-1}[1-(q/2k_F)^2]^{-1/2}\Theta(2k_F-q) \ . \tag{20c}$$

Since this expression can be written also in the form

$$\Phi_0''(\mathbf{k}_2-\mathbf{k}_1,\omega=0)=\pi\sum_{\mathbf{k}_1}\delta(\varepsilon_F-\varepsilon_{\mathbf{k}_1})\delta(\varepsilon_{\mathbf{k}_2}-\varepsilon_{\mathbf{k}_1}) \ , \tag{21a}$$

formula (20a) is equivalent to

$$1/\tau=2\pi\sum_{\mathbf{k}_2,\mathbf{k}_1}\langle\,|\,U_{sc}(\mathbf{k}_2-\mathbf{k}_1)\,|^2\rangle(1-\mathbf{k}_1\mathbf{k}_2/k_F^2)\times\delta(\varepsilon_{\mathbf{k}_1}-\varepsilon_{\mathbf{k}_2})\delta(\varepsilon_F-\varepsilon_{\mathbf{k}_1})/\rho_F \ . \tag{21b}$$

This is the known result for Drude's current relaxation rate as it follows from the kinetic-equation approach. The scattering rate is evaluated in Born approximation, but the disorder electron interaction is screened by the full wave-vector-dependent dielectric function of the Fermi liquid, Eq. (20b). Matthiesen's rule for the superposition of ion and roughness scattering holds in this approximation, Eq. (3b). The result (21b) and (20b) modifies those formulas, which have been discussed extensively in the literature (see Ref. 1) by the incorporation of local-field corrections. Scattering physics is rediscovered from Eq. (9), if the density spectrum can be written as superposition of particle- (i.e., outgoing electrons) hole (i.e., ingoing electrons) excitations, Eq. (21a). Screening is obtained, since Coulomb interaction suppresses the free spectrum by the square of the screening factor, Eqs. (2d) and (20b). Equations (20) adopt the Mott-Jones formula[37] to two-dimensional systems and generalize the latter by using a general q-dependent screening function instead of the Thomas-Fermi asymptote. Results equivalent to Eq. (20) have been obtained originally for three-dimensional systems.[30] Departures from the Mott-Jones formula due to local-field effects have been discussed in Ref. 38.

If the q dependence of U_{sc} could be neglected, i.e., if the scatterers could be considered as short ranged, $1/\tau$ would be independent of n. For the two-dimensional model of ion scatterers the q dependence of $U_{sc}(q)$ can be ignored essentially for q smaller than the screening vector q_s, Eq. (2c). So for $\xi=2k_F/q_s\ll 1$, i.e., for $n\ll 2.8\times10^{13}$ cm^{-2}, $1/\tau$ decreases only weakly with increasing n. The form factors of the layer lead, however, to an appreciable suppression of the relaxation rate if $n>10^{11}$ cm^{-2}. Local-field corrections are irrelevant for densities exceeding 10^{13} cm^{-2}. For smaller n the local-field corrections suppress the screening effects and hence they increase the relaxation rate. Local-field corrections decrease the mobility by a factor of 1.6 and 1.2 for $n=10^{11}$ cm^{-2} and $n=10^{13}$ cm^{-2}, respectively (for the realistic form factors). These results are in qualitative agreement with previous results, see Fig. 62 of Ref. 1.

For the density range $10^{12}<n$ cm$^2<10^{13}$ the theory predicts an almost linear increase of the mobility $\mu_0=e\tau/m$ with electron concentration. This result is in agreement with experimental findings of Ref. 5, as shown in Fig. 1. The quoted data were obtained by extrapolating the experimental values to $n_i\to 0$. The figure also shows the effect of taking the depletion density into account and demonstrates an assumed distance z_i between ions and interface of 2 Å, which is about 10% of the Bohr radius. Choosing $z_i\neq 0$ has only a small effect on the results for low density but a large effect for high density because then the wave function is very localized in the x direction.

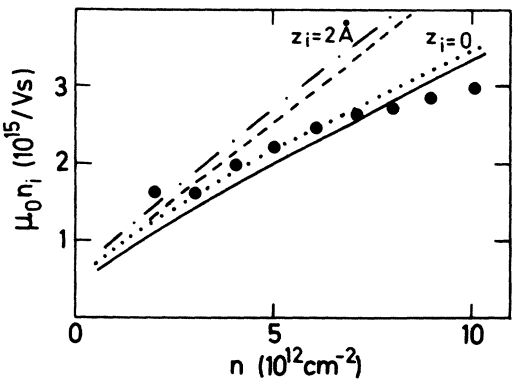

FIG. 1. Kinetic-equation result for the mobility normalized by the inverse of the impurity concentration n_i versus electron concentration n. The experimental results (dots) (Ref. 5) refer to a depletion density $N_{\rm depl}^{\rm ex}=3.6\times10^{11}$ cm^{-2}. Solid curve: $N_{\rm depl}=N_{\rm depl}^{\rm ex}$, $z_i=0$ Å; dotted curve: $N_{\rm depl}=0$, $z_i=0$ Å; dashed curve: $N_{\rm depl}=N_{\rm depl}^{\rm ex}$, $z_i=2$ Å; dashed-dotted curve: $N_{\rm depl}=0$, $z_i=2$ Å. $G\neq 0$ and $1/b\neq 0$ in all cases.

B. Mobility suppression

The zero-frequency density spectrum for the Fermi liquid without disorder vanishes in the long-wavelength limit because of the long-ranged Coulomb interaction. From Eqs. (2c), (2d), (6), and (20c), one gets

$$\Phi_c''(q\to 0,\omega=0)=\rho_F(q/q_s^2 v_F)\ . \tag{22a}$$

The excitation spectrum of the disordered system, on the other hand, approaches a nonzero constant, given by the inverse mobility $1/\mu=n/[eK''(\omega=0)]$. From Eqs. (2c) and (15a), one finds

$$\Phi''(q\to 0,\omega=0)=\rho_F(e\rho_F/(nq_s^2))/\mu\ . \tag{22b}$$

Notice that these two results are essentially exact ones; our approximation concerns the numerical values of ρ_F, q_s, and μ only. So there is a large low-frequency long-wavelength enhancement E of the density spectrum;

$$E=\Phi''(q\to 0,\omega=0)/\Phi_c''(q\to 0,\omega=0)\ .$$

It expresses the fact, that in disordered systems, particles move much slower on the average than in a zero-temperature Fermi liquid. Consequently, small momentum recoil processes are much more efficient than estimated in the lowest-order approximation and therefore one finds

$$M''(\omega=0)>1/\tau\ . \tag{22c}$$

The range in q space, where Eq. (22b) is valid, shrinks if the disorder becomes small. Hence, the relaxation enhancement is larger, the larger the disorder.[9,10] This fact is demonstrated as upward bending of a $1/\mu=(m/e)M''(\omega=0)$ versus n_i curve, as shown in Fig. 2(a), in comparison with some experiments.[5] If one wants to present the suppression effect more clearly as opposed to the variations of μ_0, one can plot $\mu/\mu_0=\sigma/\sigma_0$ versus the experimental parameter. In Fig. 3(b) this is shown for the same quantities as exhibited in Fig. 2(a).

Let us contemplate the mobility suppression for fixed n_i. If μ_0 decreases with decreasing n—because of the increasing importance of backward scattering events—also the enhancement $E=(ev_F\rho_F)/(qn\mu)$ will increase. So the deviation from linearity in Fig. 2(a) or the slope in Fig. 2(b) will become larger if n decreases, as shown by the dashed-dotted curves. Even if μ_0 does not depend on n strongly, μ will strongly suppressed with decreasing n, since the factor $v_F\rho_F/n\propto 1/\sqrt{n}$ in E increases. This is shown in Fig. 3 in comparison with data of Ref. 4. The mobility suppression shows up in a σ versus n plot, such that the curves extrapolate to zero at a value $n\to n^c>0$, Fig. 4.

It should be reemphasized that in Figs. 2, 3, and 4 the data are interpreted as a result of recoil enhancement due to disorder. The influence of disorder on the density of states ρ_F or on the compressibility $g(q)$ are neglected. The latter effects have been recently studied within the self-consistent Born approximation for point scatterers,[39]

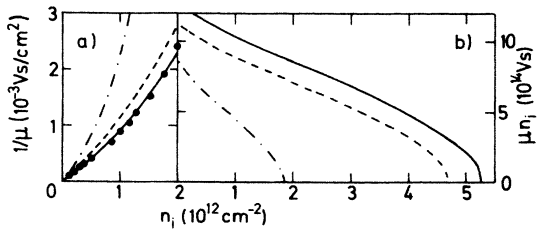

FIG. 2. (a) Inverse mobility $1/\mu$ and (b) mobility normalized by the inverse scatterer density n_i as a function of n_i for $N_{\rm depl}=3.6\times 10^{11}$ cm^{-2}. Dots are experimental results of Ref. 5 for $n=2\times 10^{11}$ cm^{-2}. Solid and dashed curves are the present theory with $z_i=2$ Å and $z_i=0$, respectively. The dashed-dotted curve is the result for $z_i=2$ Å and $n=1\times 10^{11}$ cm^{-2}.

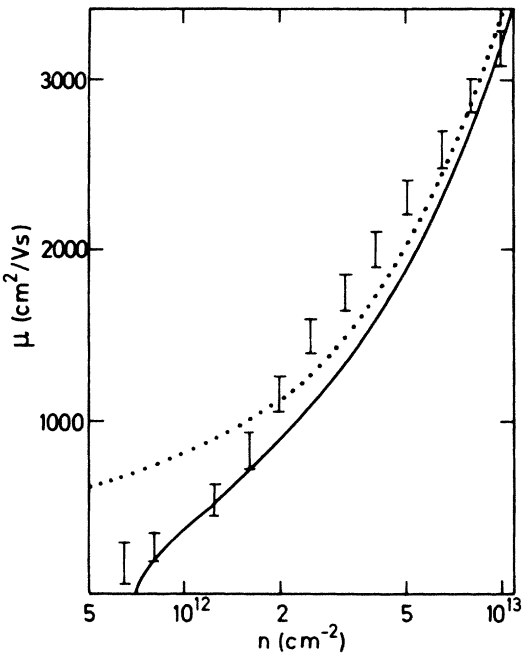

FIG. 3. Mobility μ versus electron density n for $N_{\rm depl}=3.6\times 10^{11}$ cm^{-2} and $n_i=10^{12}$ cm^{-2} (Ref. 4). Solid curve is the present theory with $z_i=0$ Å and the dotted curve is the kinetic equation-result for the mobility μ_0.

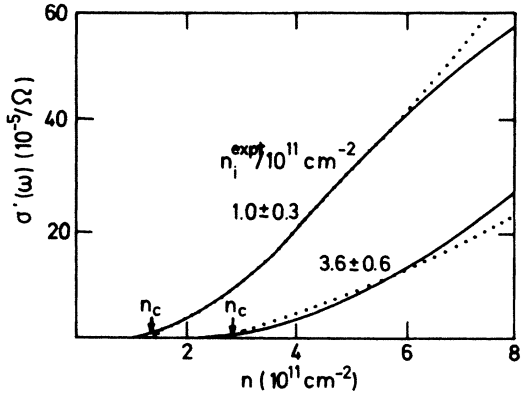

FIG. 4. Static conductivity versus density for $n_i=1.4\times 10^{11}$ cm^{-2} and $n_i=3.4\times 10^{11}$ cm^{-2} according to the present theory. Solid curves are experimental results of Gold, Götze, Mazuré, and Koch (Ref. 52) measured at $\omega=0.001$ cm^{-1}.

adapting to the two-dimensional systems earlier calculations by de Gennes[40] for bulk material. For ion scatterers a corresponding evaluation would require the solution of complicated integral equations. If the results were available, they could be incorporated in the present theory by modifying the reference functions Φ^R, g^R in Eq. (10b). One effect of this modification would be the change of the screening in Eq. (20b). Das Sharma[41] argued recently that disorder makes screening less efficient and this yields also an increase of the $1/\mu$ versus n_i curve, in agreement with the data shown in Fig. 2(a). In Ref. 41 no comparison was made with our previous work on mobility suppression[11,12] and we cannot discuss the work of Ref. 41 because no equation has yet been published.

C. Mobility edge

The self-consistency equations lead to a positive feedback between mobility suppression and enhancement of the recoil spectrum $\Phi''(q,\omega=0)$. This is easily understood if one imagines an iterative solution of Eq. (9). In the preceding section it was shown that from $1/\mu_0>0$ one gets

$$\Phi_1''(q\to 0,\omega=0)\gg\Phi_0''(q\to 0,\omega=0)=\Phi_c''(q\to 0,\omega=0)$$

and hence $\mu_1<\mu_0$. From here, Eq. (22b) yields

$$\Phi_2''(q\to 0,\omega=0)=[\rho_F^2 e/(nq_s^2)]/\mu_1>\Phi_1''(q\to 0,\omega=0)\ .$$

This leads to $1/\mu_2>1/\mu_1$, etc. The iteration stabilizes because of the large q contributions to the decay integral, Eq. (9), where the asymptotic expansions (22a) and (22b) are invalid. This, however, holds only if the disorder is not too large. There is a critical value for the disorder where $M''(\omega=0)$ diverges; at this critical value the mobility continuously approaches zero, as shown by the curves in Figs. (2b), 3, and 4. If the disorder exceeds the critical value, the relaxation kernel exhibits a zero-frequency pole: $M(z)=-s/z$, $s>0$. Hence, the polarizability $\chi(z)=e^2K(z)/z$, the response function for the dipole moment induced by an homogeneous field,[27] assumes a finite static value $\chi=\chi(z=i0)$:

$$\chi=e^2n/(ms)\ . \tag{23a}$$

So for strong disorder the system is an insulator. Approaching the critical disorder from the insulator side, χ diverges. Connected with the pole of the relaxation kernel in the insulator is a corresponding one for the density propagator. From Eq. (15a), one gets

$$\Phi(\mathbf{q},z=0)=\frac{-1}{z}g_c(\mathbf{q})/\{1+[nq^2/msg_c(\mathbf{q})]\}\ . \tag{23b}$$

Hence, density fluctuations, once created, do not vanish for large times $\Phi''(q,\omega\to 0)\propto\delta(\omega)$. The electrons are localized in the insulator. The condition for the conductor-insulator transition can be formulated in terms of the dimensionless coupling constant of the theory

$$A=\sum_{\mathbf{q}}\langle\,|U(\mathbf{q})|^2\rangle g_c(\mathbf{q})^2/(2n^2)\ . \tag{24}$$

If $A<1$, the system is a conductor, i.e., $\mu>0$, $1/\chi=0$. If $A>1$, the system is an insulator, i.e., $\mu=0$ and $1/\chi>0$. A depends on all the parameters of our model like, e.g., n, n_i, and N_{depl}. The condition $A=1$ defines the hypersurface in the parameter space separating the conductor from the insulator. All the preceding statements hold in complete correspondence and can be shown in detail, in complete analogy to the corresponding ones discussed before for noninteracting particles moving in a random potential.[9,10]

In Fig. 5 the phase-separation line in a $\ln n_i$ versus $\ln n$ plot is shown for varius model assumptions (roughness scattering ignored). One should notice the obvious properties, that incorporation of the form factors, $1/b\neq 0$, and the introduction of a separation between impurities and electrons, $z_i\neq 0$, favors the conductor. Inclusion of local-field corrections favors localization. For the range of experimental interest, $10^{11}<n_i\ \text{cm}^2<10^{12}$, the effects of F, F_i, and G on the transition point can be incorporated in renormalizing n_i to some effective value n_i^{eff}. The power-law relation between n_i and n, demonstrated approximately in the diagram, can be understood if one evaluates A in the limit $\xi=2k_F/q_s\ll 1$ for the model without form factors. One finds

$$A=[n_i/(n\xi^{2/3}g_v)][1-(2g_v)^{-1}]^{-4/3}[\pi/(12\sqrt{3})2^{4/3}]\ ;$$

the second bracket accounts for the local-field corrections. Hence, the critical impurity density is given as

$$n_i^c=n\,[n^{1/2}\bar{\epsilon}/(e^2m)]^{2/3}n_0,\quad \xi\ll 1\ . \tag{25}$$

Here, n_0 is a constant absorbing the effects of $G\neq 0$, $z_i\neq 0$, and $1/b\neq 0$. The strange exponent $\frac{4}{3}$ of n, entering the transition criterion, reflects the singular space dependence of the screening clouds, surrounding the impurities. In Fig. 6 the critical impurity density as obtained from the present theory, the solid curve in Fig. 5, is compared with the asymptotic law given by Eq. (25) and

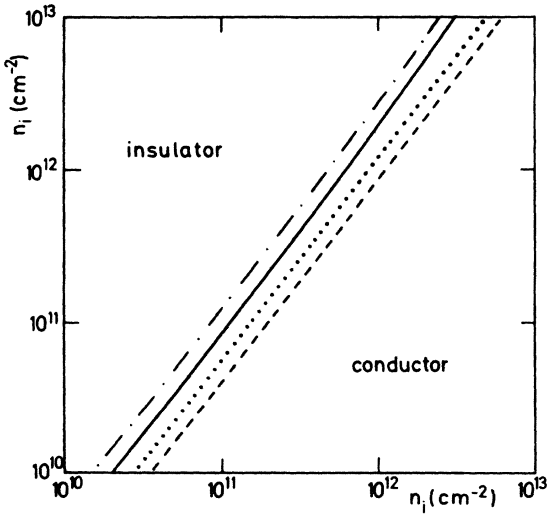

FIG. 5. Conductor-insulator transition lines for $N_{\text{depl}}=0$. Solid and dashed-dotted curves are for $1/b\neq 0$ and $G\neq 0, G=0$, respectively. Dashed and dotted curves for $1/b=0$ and $G\neq 0, G=0$, respectively (all curves are for $z_i=0$).

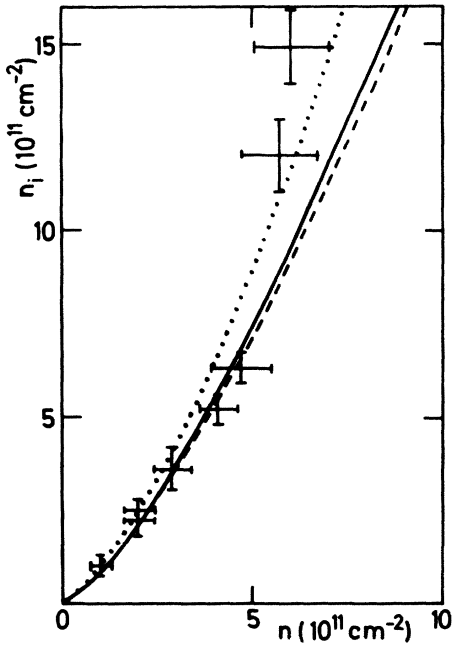

FIG. 6. Critical impurity density n_i^c as a function of electron density n for $n_{\text{depl}}=0$ (Ref. 42). The solid curve is the result of the present theory with $z_i=0$. The dotted curve is for $z_i=5$ Å and the dashed curve is the asymptotic law according to Eq. (25).

with experimental results obtained by Mazuré and Koch[42] for an accumulation layer. The experimental error bars also account for the rounding of the transition due to nonzero temperature effects.

D. Roughness scattering

The reasoning concerning the mobility suppression due to self-consistency effects obviously holds also for roughness scattering. Studies of the results for a model specified by Eq. (3d) were presented earlier.[12]

With increasing density, the mobility first increases due to screening effects but later decreases due to surface roughness scattering (see Ref. 1). Figure 7 demonstrates the effect for a μ versus n plot in comparison with some data. System parameters were chosen close to the ones used in Ref. 43, where data of Kawaji have been analyzed. Matsumoto and Uemura[43] reported that the data were incompatible with the assumption of a summation of ion scattering rate and roughness scattering rate, and therefore a third relaxation mechanism was introduced to account for the experiment. It was also argued[43] that scattering by bulk impurities was necessary to account for the data in the low-n region. Most interesting is the strong suppression of μ for $n<2\times10^{11}$ cm^{-2} where no experiments are available.

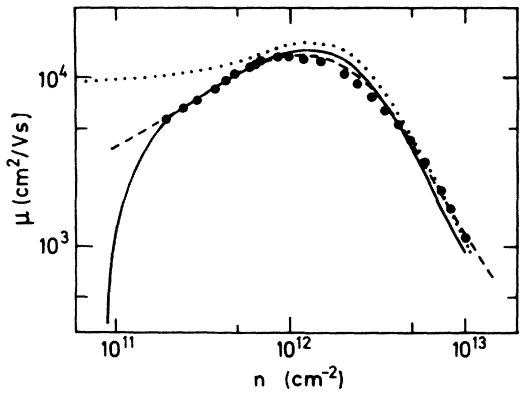

FIG. 7. Mobility versus density measured by Kawaji (Ref. 43) (dots). Dashed curve is the theoretical result of Ref. 43 for three scattering mechanisms. The solid curve is the present theory using impurity scattering and surface roughness scattering. The dotted curve is our zero-order result ($n_i=0.5\times10^{11}$ cm^{-2}, $N_D=3.6\times10^{11}$ cm^{-2}, $\Delta=2.8$ Å, $\Lambda=13$ Å).

E. Depletion field effects

The extent of the wave functions perpendicular to the interface can be decreased by increasing the depletion field. Then, the electrons are pushed to the interface and are affected more strongly by the impurity potential than before. So for fixed n_i the metallic regime shrinks and for $N_{\text{depl}}\to\infty$ we get the results for $F=F_i=1$. In Fig. 8 the static conductivity is shown as a function of N_{depl} for various electron densities and fixed n_i. The parameters should be realizable in experiment. The theory predicts a metal-insulator transition for $n=3\times10^{11}$ cm^{-2} and $n_i=3\times10^{11}$ cm^{-2} at $N_{\text{depl}}=3\times10^{11}$ cm^{-2}.

F. Plasmon excitation anomalies

Let us consider the dynamical conductivity normalized by its dc value, $\hat{\sigma}=\sigma(\omega)/\sigma$, as a function of the normalized frequency $\hat{\omega}=\omega[\sigma m/(ne^2)]$. If Drude's theory were valid, i.e., if the current relaxation kernel would be frequency independent, Eqs. (7) and (8a) would yield $\hat{\sigma}_1=\hat{\sigma}_D=1/(1+\hat{\omega}^2)$. So the kinetic-equation approach predicts all normalized conductivity curves to be a standard Lorentzian, no matter what the dynamics of the elec-

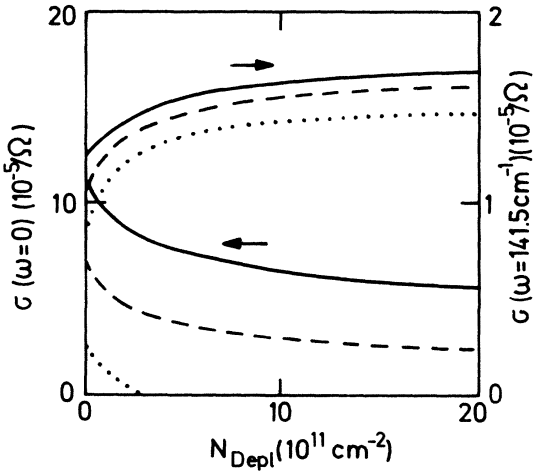

FIG. 8. Conductivity versus depletion density for $n_i=3\times10^{11}$ cm^{-2}. The solid, dashed, and dotted lines are for $n=5\times10^{11}$ cm^{-2}, $n=4\times10^{11}$ cm^{-2}, and $n=3\times10^{11}$ cm^{-2}, respectively. Lower curves and right scales are dc values; upper curves and left scales are dynamic conductivities for $\omega=141.5$ cm^{-1}.

tron system is like. Deviations of the true dynamics from the one anticipated within the kinetic-equation approach can be seen if one compares a $\hat{\sigma}$ versus $\hat{\omega}$ plot with the standard Lorentzian. One gets

$$\hat{\sigma}(\hat{\omega})=\hat{M}''(\hat{\omega})/\{[\hat{\omega}+\hat{M}'(\hat{\omega})]^2+[\hat{M}''(\hat{\omega})]^2\} . \quad (26)$$

Within the present theory the dynamical anomalies are discussed more adequately as deviations of the normalized relaxation spectrum,

$$\hat{M}''(\hat{\omega})=M''(\omega)\sigma m/(ne^2)=M''(\omega)/M''(\omega=0) ,$$

from unity. Frequency dependencies of $M''(\omega)$ cause $M'(\omega)\neq 0$ via a Kramers-Kronig relation, and this reactive part of the kernel also enters the dynamical conductivity for $\omega\neq 0$.

The lowest-order result for the relaxation spectrum $M_0''(\omega)$, Eq. (19), exhibits a strong frequency dependence, since the Coulomb interactions imply a strong frequency dependence of the density of states for density excitations $\sum_{\mathbf{q}}\Phi_c''(q,\omega)$. Let us rewrite the result with the aid of Eq. (20) in the form

$$M_0''(\omega)=\sum_{\mathbf{q}} q^2\langle\,|\,U_{sc}(\mathbf{q})\,|^2\rangle R(\mathbf{q},\omega)\Phi_0''(\mathbf{q},\omega)/2nm + \sum_{\mathbf{q}} q^2\langle\,|\,U(\mathbf{q})\,|^2\rangle r(\mathbf{q})\pi\delta(\omega-\omega_p(q))/2nm . \quad (27)$$

Here, the strength factor for the plasmon excitation is given by

$$r(\mathbf{q})=1/[v_{\mathrm{eff}}(q)^2\omega_p(q)\delta\chi_0'(\mathbf{q},\omega_p(q))/\delta\omega]$$

and

$$R(\mathbf{q},\omega)=|\,[1+g_0(\mathbf{q})v_{\mathrm{eff}}(q)]/[1+\chi_0(\mathbf{q},\omega+i0)v_{\mathrm{eff}}(q)]\,|^2 .$$

For the model $F=F_i=1$, $n=5\times10^{11}$ cm^{-2}, $n_i^{\mathrm{eff}}=1.2\times10^{11}$ cm^{-2}, the various contributions to $M_0''(\omega)$ are shown in Fig. 9. There is some frequency variation of $M_0''(\omega)$ due to the frequency dependence of $\Phi_0''(q,\omega)$. This part reflects phase-space variations of the two-dimensional particle-hole excitations, and it is obtained by dropping the plasmon contribution in Eq. (27) and putting $R(q,\omega)\cong R(q,\omega=0)=1$; it is shown by the dotted curve. This is the only contribution which occurs also for the model of noninteracting electrons moving in a screened random potential $U_{sc}(\mathbf{q})$, Eq. (20b). If $R\neq 1$ is observed, the dashed-dotted curve in Fig. 9 is found and $M_0''(\omega)$ rises with increasing ω in the frequency domain of interest. Incorporation of R is equivalent to including the frequency dependence of the screening function. With increasing ω, screening becomes less efficient, leading to an enhancement of the relaxation rate. If the plasmon contribution is added, the dashed curve in Fig. 9 is obtained. For small ω, only small-q contributions enter and so long-wavelength expansions can be used to derive, as a plasmon excitation contribution

$$M_{0,p}''(\omega\to 0)=\varepsilon_F(\omega/\varepsilon_F)^5[\pi n_i/(8ng_v)](k_F/q_s)^2 . \quad (28)$$

Hence, current relaxation due to plasmon excitation leads to a considerable increase of $M_0''(\omega)$ with increasing frequency; the relaxation spectrum acquires a pronounced peak. Even if the electron impurity interaction effect is so large as to yield an almost 50% reduction of μ as compared to μ_0, the effect still survives, as shown by the solid curve in Fig. 9. In Fig. 10 the influence of various model parameters on the relaxation spectrum is displayed. Notice that the introduction of form factors, $1/b\neq 0$, leads to a strong suppression of the large frequency relaxation rate in comparison with the one for a model with $F=F_i=1$.

The strong variations of the relaxation spectrum lead to the following anomalies of the conductivity. For large frequencies, an enhancement of the spectrum is predicted:

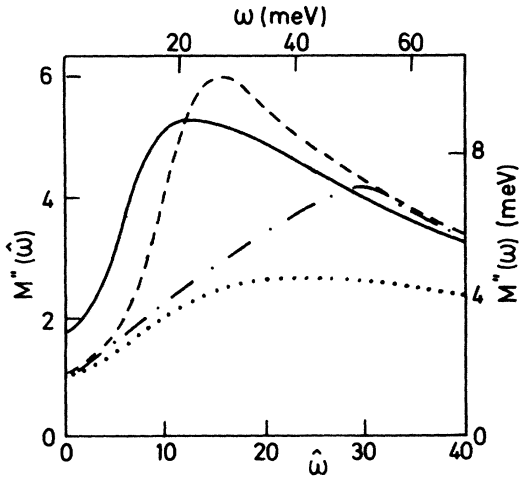

FIG. 9. Normalized relaxation spectrum M'' as a function of normalized frequency, see text.

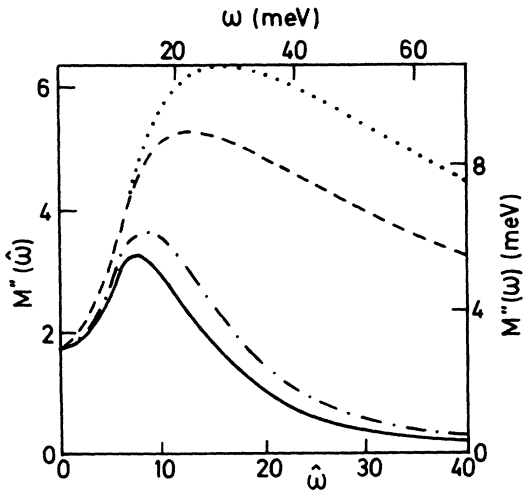

FIG. 10. Normalized relaxation spectrum as a function of the normalized frequency for $n=5\times10^{11}$ cm^{-2} and n_i chosen to give the same dc value. Solid and dashed-dotted curves are for $1/b\neq 0$ and $G\neq 0$, $G=0$ ($n_i=2.25\times10^{11}$ cm^{-2}, $n_i=3.15\times10^{11}$ cm^{-2}), respectively. Dashed and dotted curves are for $1/b=0$ and $G\neq 0$, $G=0$ ($n_i=1.2\times10^{11}$ cm^{-2}, $n_i=1.75\times10^{11}$ cm^{-2}), respectively. All curves are for $N_{\mathrm{depl}}=0$.

$$\hat{\sigma}(\hat{\omega})=\hat{M}''(\hat{\omega})/\hat{\omega}^2,\quad \omega \gg |M(\omega)|\ . \tag{29a}$$

The f-sum rule requires a corresponding small frequency suppression of the current spectrum below the Drude curve:

$$\hat{\sigma}(\hat{\omega})=1-[\hat{M}''(\hat{\omega})-1]-[\hat{\omega}+\hat{M}'(\hat{\omega})]^2,\quad \hat{\omega}\ll\hat{M}(\hat{\omega})\ . \tag{29b}$$

Notice that the suppression is also determined by the reactive part $\hat{M}'(\hat{\omega})$. The tail enhancement due to plasmon emission was discussed originally for bulk metals for an approximation corresponding to $M\cong M_0$.[30] In bulk materials it is necessary for ω to exceed $\omega_p=(4\pi n_b e^2/m)^{1/2}$ where n_b is the electron number per volume. This frequency is rather large and so the anomalies show up only far out in the Drude tail. In two-dimensional systems the anomaly already sets in at low frequencies and so the whole effect is more important, as was pointed out by Tzoar, Platzman, and Simons in a discussion of plasmon damping for electron layers;[44] these authors examined a formula equivalent to Eq. (29a) with $M\cong M_0$.

A side remark might be helpful. The kinetic-equation approach, or better, the extension of the random-phase approximation by inclusion of a Drude damping is obtained by writing $\tilde{M}(z)=iM''(0)$ in Eq. (13). Such an approximation was analyzed[45] for bulk systems. When the Mermin[45] formula for the density propagator is used in the calculation of the relaxation kernel in Eq. (9), one gets a first nonlinear correction to the lowest-order approximation of our theory.

Equation (29a) can be written as $\sigma(\omega)=\sigma_D\alpha$, where

$$\sigma_D=[e^2/(m\omega)^2](n/\mu_0)$$

is the conductivity predicted by the Drude law, while $\alpha=M''(\omega)/M_0''(0)$ is the enhancement factor due to plasmon excitations. σ_D is a monotonically increasing function of n if we are sufficiently above the conductor-insulator transition; for large n there is a tendency for σ_D to become n independent (Fig. 3). With increasing n the plasmon frequency increases; $\omega_p(q)\propto\sqrt{nq}$ for $q\to 0$. This stiffening of the modes decreases the excitation phase space; $M''_{0,p}(\omega)\propto\omega^5/n^2$ in Eq. (28). Hence, α will decrease with increasing n till the whole enhancement gets lost, for sufficiently large n. The decrease of α can overcompensate for the increase of σ_D, so that the $\sigma(\omega)$ versus n curve for $\omega\neq 0$ exhibits a maximum, Fig. 11. Thus, the nonmonotonic $\sigma(\omega)$ versus n behavior[8] is explained by the present theory. The measurement of α is a rather direct detection of the plasmon density of states. We mention that finite-thickness effects of the electron layer increases the peak structure (see Fig. 11). For $1/b=0$, the self-consistent calculation of $M(\omega)$ is necessary to account for the experiments reported by Gold, Götze, Mazuré, and Koch.[46]

G. Plasmon damping and plasmon shifts

In the long-wavelength limit, the Green-Kubo identity (15a) is the most convenient formula for a qualitative study of the damping and shift of the plasmon resonance. Using Eq. (8a), the normalized spectral function reads

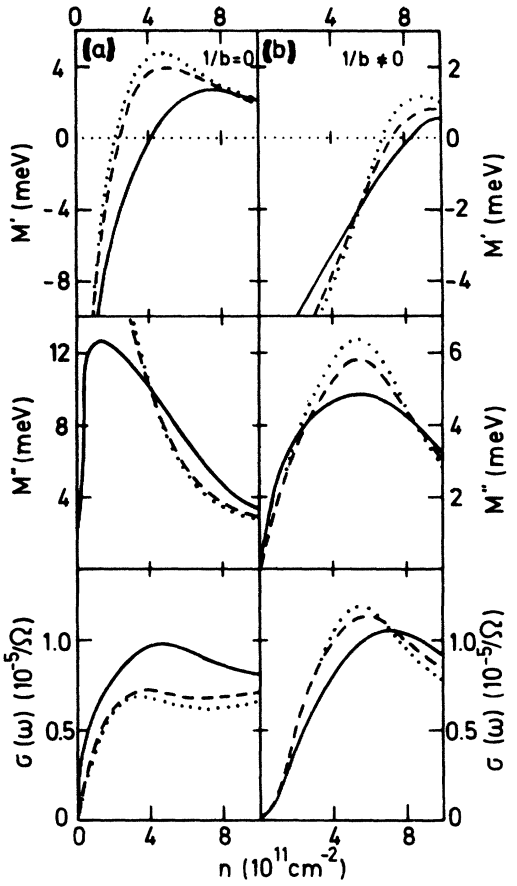

FIG. 11. M', M'', and σ' as a function of electron concentration n for $N_{\rm depl}=0$, $\omega=141.6\ {\rm cm}^{-1}$. The solid curves are due to the present theory, the dashed curves are obtained by using the Mermin formula (Ref. 45) in Eq. (9), and the dotted curves are the frequency-dependent zero-order results. (a) $1/b=0$, $n_i=1.2\times10^{11}\ {\rm cm}^{-2}$; (b) $1/b\neq 0$, $n_i=2.25\times10^{11}\ {\rm cm}^{-2}$.

$$\Phi''(\mathbf{q},\omega)/g_c(\mathbf{q})=\omega_p^2(q)M''(\omega)/\{[\omega^2-\omega_p(q)^2+\omega M'(\omega)]^2+\omega^2[M''(\omega)]^2\}\ . \tag{30}$$

Here, $\omega_p(q)=[nq^2/mg_c(q)]^{1/2}$ is the plasmon dispersion, Eq. (2e), of the system without disorder. Formula (30) is the characteristic absorption of an oscillator coupled to other degrees of freedom, whose reaction on the oscillator is described by the polarization operator $M(z)$. If $\omega_p(q)$ is not too small, i.e., for a q larger than some characteristic q^*, $\Phi''(q,\omega)$ will exhibit a nonzero frequency peak at $\Omega(q)$ of a characteristic half-width at half height $\Gamma(q)$. $\Omega(q)$ is the true plasmon dispersion of the system and $\Gamma(q)$ is the plasmon damping. For $q<q^*$ propagating modes do not exist, the oscillations are overdamped; $\Phi''(q,\omega)$ exhibits a maximum at zero frequency.

Within Drude's theory $M(\omega+i0)=iM''(\omega=0)$ and Eq. (30) describe an oscillator with constant friction. Therefore, one expects a q-independent damping given by the mobility

$$\Gamma_D=\tfrac{1}{2}M''(\omega=0)=e/(2m\mu)\ . \tag{31}$$

Connected with the damping is a downward shift of the resonance, which, however, is a quadratic effect in the

damping constant:

$$\Omega_D(q)=\omega_p(q)[1-2\Gamma^2/\omega_p^2(q)]^{1/2} .$$

The resonance disappears for $q_D^*=(2m/q_s\varepsilon_F)\Gamma_D^2$. The above results have been discussed recently.[47] The Drude results are wrong, even in the limit $\omega\to 0$, $q\to 0$. For small frequencies one can write

$$M'(\omega)=\gamma\omega+O(\omega^2) , \tag{32a}$$

and so one finds

$$\Omega(q)=\omega_p(q)/\sqrt{(1+\gamma)} , \tag{32b}$$

$$\Gamma=\Gamma_D/(1+\gamma) , \tag{32c}$$

$$q^*=q_D^*/(1+\gamma) . \tag{32d}$$

These formulas hold as long as $M''(\omega)$ does not vary appreciably with frequency on the scale Γ, $\Omega(q)$. The plasmon emission anomaly for large frequencies causes a normal dispersion for $M'(\omega)$ at low frequencies and this leads to a $\gamma>0$, see Fig. 11. Hence there is a plasmon softening, $\Omega(q)/\omega_p(q)<1$, which is a linear effect in Γ_D. It is connected with a sharpening of the resonance, $\Gamma<\Gamma_D$, and a corresponding shrinking of the regime for overdamping, $q^*<q_D$.

If the plasmons are well defined, $\omega_p\gg M''(\omega)$, an expansion of the denominator around $\Omega(q)$ brings out

$$\Omega(q)^2=\omega_p(q)^2-\Omega(q)M'(\Omega(q)) \tag{33a}$$

and

$$\Gamma(q)=\tfrac{1}{2}M''(\Omega(q))\Big/\left[1+\frac{1}{2\Omega(q)}\left[M'(\Omega(q))+\frac{\partial M'(\Omega(q))}{\partial\omega}\right]\right] . \tag{33b}$$

The resonance structure of $M''(\omega)$ implies that $M'(\omega)$ changes sign, Fig. 11. Hence, for larger ω, the disorder causes an increase of the resonance $\Omega(q)>\omega_p(q)$. Before entering this regime, the damping increases considerably above Γ_D. To discuss the large frequency plasmon properties correctly, Eq. (3a) cannot be used and we will apply our approximation (13). In Fig. 12 plasmon shifts and broadening, as obtained from our theory, are shown; the results of the Mermin[45] formula are shown as dashed curves. The dotted curve in Fig. 12 represents[47]

$$\Omega/\omega_p=[1-(M_0'')^2/4\omega_p^2]^{1/2} .$$

In Fig. 13 a representative set of density spectra is exhibited in order to elucidate the influence of disorder on the dynamical structure factor of MOS systems. Figure 14 exhibits the impurity density dependence of the plasmon frequency renormalization together with $M''(\omega)$ at the plasmon frequency. The dotted curve refers to the same as in Fig. 12 and to $M_0''(0)/\omega_p$, respectively.

There are experiments showing our effect qualitative-

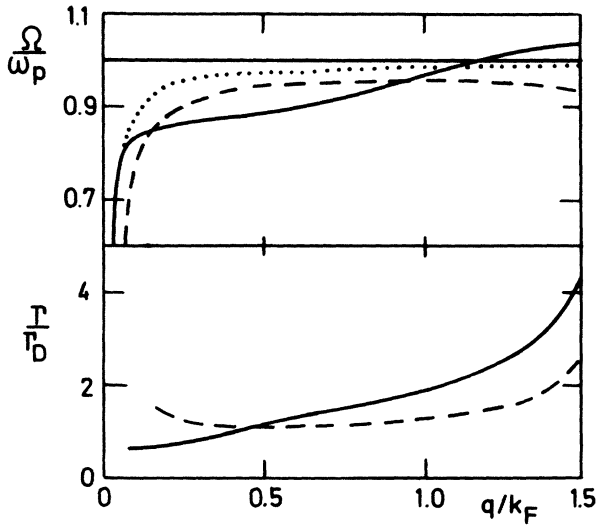

FIG. 12. Plasma resonance Ω relative to the Fermi-liquid value ω_p (determined numerically) and plasma damping Γ for $n=5\times10^{11}$ cm^{-2}, $n_i=2.25\times10^{11}$ cm^{-2}, $N_{\text{depl}}=0$, and $1/b\neq0$ versus wave vector q in units of k_F. The dashed curves are the kinetic-equation results, and for the dotted curve, see text.

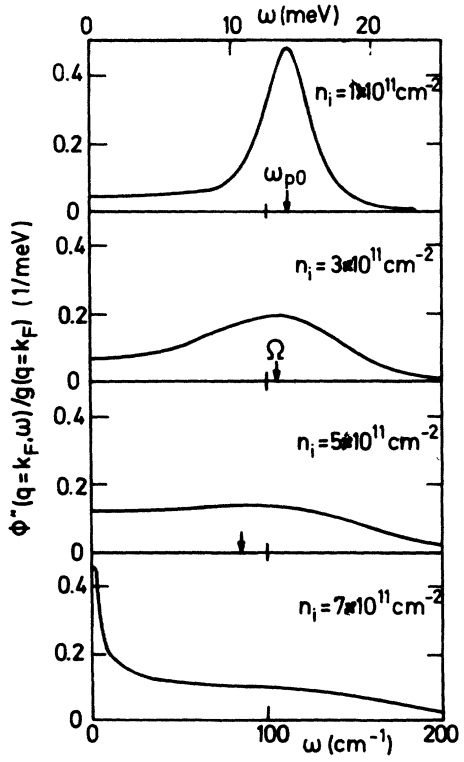

FIG. 13. Density spectrum normalized to the compressibility as a function of frequency for $q=k_F$, $n=5\times10^{11}$ cm^{-2}, and for various impurity densities n_i ($N_{\text{depl}}=0$, $1/b\neq0$).

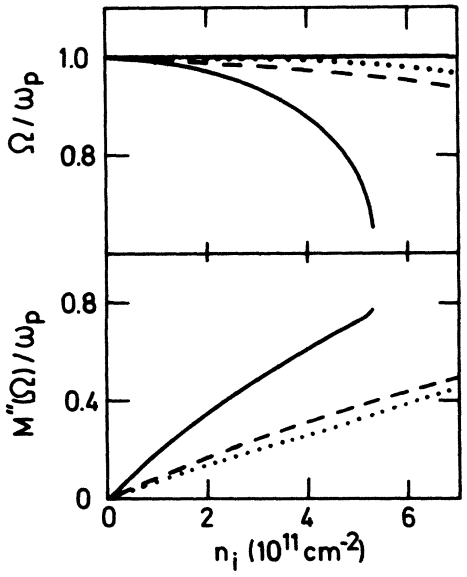

FIG. 14. Plasma frequency Ω and $M''(\Omega)$ versus impurity density. Solid curves are for $n=5\times10^{11}$ cm^{-1} and $q=k_F$ and dashed curves are for $n=10^{12}$ cm^{-2} and $q=\frac{1}{4}k_F$. For the dotted curves, see text. ($N_{\rm depl}=0$, $1/b\neq0$.)

ly.[48,49] A quantitative comparison between theory and experiment is not possible, since the mentioned work does not deal with specified Na^+ contamination.

H. A very-low-frequency singularity

If frequencies and wave vectors are so small that $M''(\omega)$ can be considered as ω independent and $|\omega M''(\omega)|$ and ω^2 are small compared to $M''(0)^2$, Eq. (30) reads

$$\Phi''(\mathbf{q},\omega)/g_c(\mathbf{q}) = [\omega_p(q)^2/2\Gamma_D]/\{\omega^2+[\omega_p(q)^2/2\Gamma_D]^2\} . \quad (34)$$

So the density spectrum is a central Lorentzian whose width ω_H is given by the mobility μ, Eq. (31),

$$\omega_H = q(q_s\varepsilon_F\mu/e) . \quad (35)$$

Let us remember that for noninteracting particles the Green-Kubo formula yields for the normalized low-frequency long-wavelength density spectrum $Dq^2/[\omega^2+(Dq^2)^2]$, with D denoting the diffusivity $D\propto\mu$. So the excitation, discussed in Sec. IV F as overdamped plasmon, can also be described as diffusion mode. But there is a wave-vector-dependent diffusivity $D(q)=(q_s/q)(\varepsilon_F\mu/e)$, which diverges for $q\to0$. The strong singularity exhibited by $\Phi''(q,\omega)$ for $\omega\to0$ and $q\to0$ leads to a singular low-frequency contribution to the relaxation kernel. This singularity, obtained from the $q\to0$ contribution to Eq. (9) reads for $\omega\to0$

$$M_s''(\omega)=a\omega^2\ln|\omega| , \quad (36a)$$

where in leading order in n_i one finds

$$a=[n_i/(4ng_v)](m/q_s^2)[g_ve^2/(n\sigma)]^3 .$$

The self-consistency yields an enhancement of a with decreasing σ. Consequently, the current decay into anomalous diffusion modes or, equivalently, into overdamped plasmons, leads to a decrease of the relaxation spectrum $M''(\omega)$ with increasing ω. This effect is opposite in its trend to the anomaly due to decay into well-defined plasmons, which is discussed in Sec. IV F. For small enough frequencies the singularity $M_s(\omega)$ always dominates. The reactive part, corresponding to Eq. (36a), reads $M_s'(\omega)=a\omega|\omega|$. Substitution of $M_s(z)$ into Eqs. (7) and (8a) yields a corresponding singularity for the dynamical conductivity at very low frequencies

$$\sigma(\omega)=\sigma[1-(am\mu/e)\omega^2\ln|\omega|+O(\omega^2)] . \quad (36b)$$

As a result of the mode coupling equation (9) and the Green-Kubo formula (15a), we arrive at the following predictions. Opposite of the outcome of the Drude law, the low-frequency conductivity will rise with increasing frequency. $\sigma(\omega)$ will show a maximum at some frequency $\omega_m\neq0$ before it decreases. $[\sigma(\omega)-\sigma]/\omega^2$ should not approach a constant for $\omega\to0$, as implied by the Drude law, but it should diverge logarithmically. The strong plasmon excitation anomaly, explained in Sec. IV E, restricts the frequency range of the asymptotic formula (36b) to a very narrow one. But Fig. 15 demonstrates that an experimental verification should be possible with MOS devices. A side remark might be in order. The Drude theory predicts currents to decay exponentially in time $j(t)/j(t=0)=K(t)/K(t=0)=\exp(-t/\tau)$, where $K(t)$ is the Laplace back transform of $K(z)$. The formula (36b) implies instead

$$K(t)=-(2am\sigma\mu/e^2)/|t|^3+O(1/|t|^4) . \quad (36c)$$

So for long times the currents decay only algebraically and, actually, they have the opposite direction from that at time zero. The singularity discussed above is yet another example of a long-time anomaly due to coupling of an observable to a hydrodynamic mode (see Ref. 50 for a review).

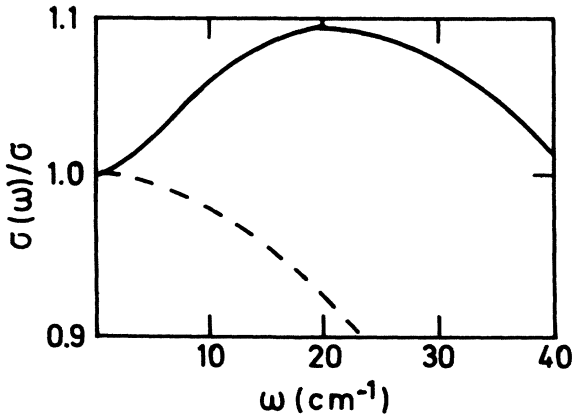

FIG. 15. Normalized conductivity as a function of frequency for $n=2.5\times10^{11}$ cm^{-2}, $n_i=2.25\times10^{11}$ cm^{-2}, $N_{\rm depl}=0$, and $1/b\neq0$. The dashed curve is the Drude result. ($\sigma_0=2.86\times10^{-5}/\Omega$.)

I. Current spectra

The relaxation enhancement due to the slowing down of the particle motion is disordered environments, discussed in Sec. IV B, is most pronounced for small ω. If ω is comparable or even larger than $|M(\omega)|$, the recoil spectrum $\Phi''(q,\omega)$ is close to the one for the system without disorder $\Phi_c''(q,\omega)$. Actually, $\Phi''(q,\omega)$ even falls below $\Phi_c''(q,\omega)$, a trend required also by the sum rules (17b) and (17c). Thus, the feedback between current relaxation and recoil enhancement leads to a peak of $M''(\omega)$, centered around $\omega=0$. The singularity, discussed in Sec. IV H, was the beginning of this phenomenon well into the conductor phase. The conductor-insulator transition is characterized by the peak height as diverging. Figure 16 exhibits the quantitative details for an accumulation layer. Let us emphasize that the plasmon excitation anomaly, explained in Sec. IV F, works against the appearance of the low-frequency peak in $M''(\omega)$. It shrinks the frequency range where the peak dominates, and that is the reason why it is not visible for $n > 3\times10^{11}$ cm^{-2} on the scales used in Fig. 16. The strong positive reactive part $M'(\omega)$, caused for small frequencies by the plasmon emission, cannot be overcompensated for by the negative contribution due to the localization precursor, unless one is rather close to the Anderson transition. The plasmon emission anomaly causes a kink in the M' versus ω curve near the critical point, as shown for $n=2.5\times10^{11}$ cm^{-2} in Fig. 16. In the Fermi-glass phase the relaxation spectrum exhibits a quasigap at low frequencies and the low-frequency part of $M'(\omega)$ is dominated by the non-ergodicity resonance, as shown by the dashed curves in the figure. Notice that for the insulator a considerable fraction of the M''-sum rule, Eq. (18a), is exhausted by the static contribution $M''(\omega\to0)=\pi s\delta(\omega)$, which is not shown in Fig. 16.

The localization precursors show up as minima centered around $\omega=0$ in the current spectra $\sigma(\omega)$. These minima are suppressed considerably as compared to the ones predicted originally for noninteracting electrons[11,13] because of the plasmon emission anomalies. Therefore, the maximum at $\omega_m\neq0$, which the conductivity σ versus ω plot exhibits in any case, shows up on the scales used in Fig. 17 only for $n\leqq3.0\times10^{11}$ cm^{-2}. The glass spectra show a quasigap at low frequencies. $\sigma(\omega)$ for $n<n_c$ ($=2.3\times10^{11}$ cm^{-2} in Fig. 16) describes the averaged spectrum for localized particles. A particle in its trap will have a discrete spectrum, but since different particles have different traps and thus different spectra, $\sigma(\omega)$ shows a continuous distribution. In the glass $\sigma(\omega)$ reflects inhomogeneous line broadening of localized anharmonic oscillations. The low-frequency conductivity $\sigma(\omega)$ near the transition point can be evaluated analytically and is given by a dynamical scaling law.[10] But the various scaling laws do not show up on the scales displayed here and they are irrelevant for discussion of the experiments analyzed in this paper. Therefore, we will not dwell on these properties.

$\sigma(\omega)$ was reported by Gold, Götze, Mazuré, and Koch[46] for accumulation layers for five frequencies in the far infrared by absorption of laser radiation. From the data of $\sigma(\omega)$ versus n (Ref. 46), one can extract the five experimental points displayed for each spectrum in Fig. 17.

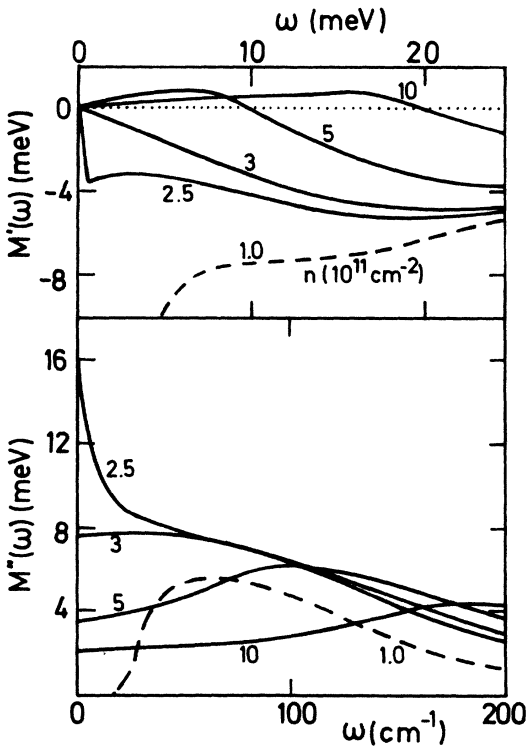

FIG. 16. Relaxation kernel M' and M'' as a function of frequency for $n_i=2.6\times10^{11}$ cm^{-2} and various densities n. The critical density is $n_i=2.3\times10^{11}$ cm^{-2}. The dashed curves refer to the insulator ($N_{\rm depl}=0$, $1/b\neq0$).

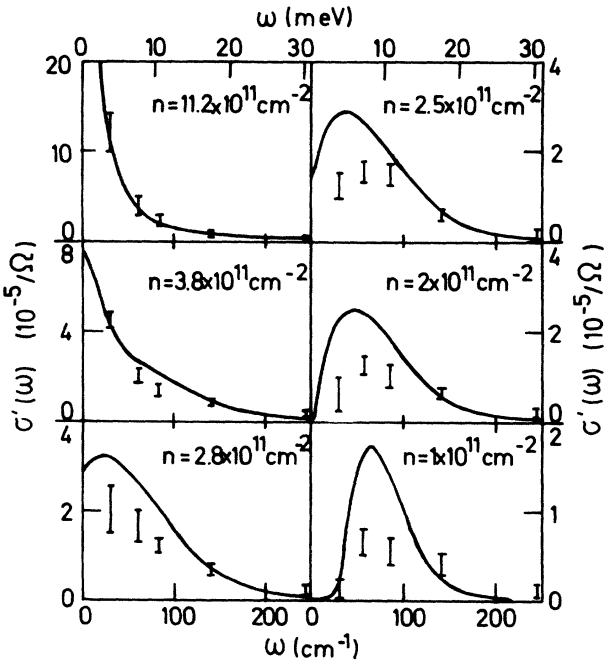

FIG. 17. Conductivity versus frequency for the same parameters as in Fig. 18. The bars are experimental results of Mazuré and Koch (Ref. 42).

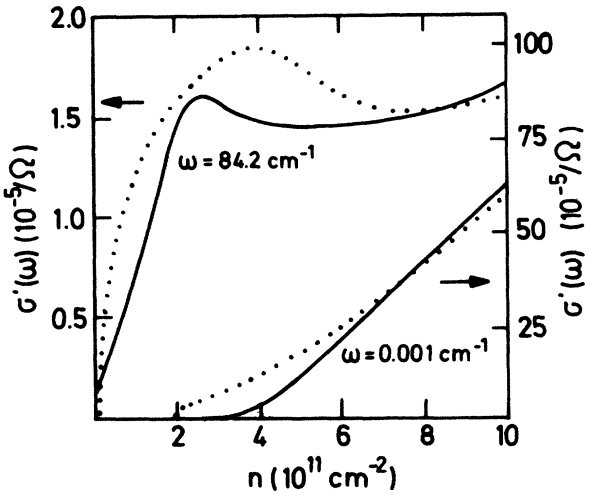

FIG. 18. Conductivity versus density for $\omega=0.001$ cm^{-1}, $\omega=84.2$ cm^{-1} as dotted lines for $n_i=2.1\times10^{11}$ cm^{-2}, $N_{\rm depl}=0$ and $1/b\neq0$. The solid curves are experimental results of Gold, Götze, Mazuré, and Koch (Ref. 52) for $n_i^{\rm exp}=(2.2\pm0.3)\times10^{11}$ cm^{-2}.

The theory is in qualitative accord with the facts, as far as the low-frequency-spectrum suppression and the large frequency enhancement due to plasmon emission anomaly are concerned. Also, the optical quasigap for low frequencies in the glass is explained. Suprisingly, the model with $F=F_i=1$ gives better agreement with the experiments than the more realistic model with F_i and F, as in Eq. (4). The discrepancies between theory and experiment are larger for smaller densities. The reason for this behavior can be seen in Fig. 10 where $M''(\omega)$ is shown as a function of frequency for various model approximations. With a finite extension of the wave function, the relevant frequency scale for $M(\omega)$ becomes smaller and so the peak structure in the conductivity increases. Perhaps intersubband excitations are possible for such strongly disturbed systems and one should take two bands into account for a more realistic description of the system.[51]

For a comparison of the theory with static and dynamic measurements, see Fig. 18, where the data of Gold, Götze, Mazuré, and Koch[52] are given. The nonmonotonic variation of the dynamical conductivity with electron density[8] is well described by the theory.

V. CONCLUSION

In the present work we studied the transport properties of an interacting electron system, which is strongly disturbed by charged impurities. Within our framework some earlier concepts are connected.

First, the idea[9] for a self-consistent calculation of the density and current relaxation gives a nonlinear n_i dependence of the transport properties (Fig. 3), a transition from a metal to an insulator (Fig. 6), and a non-Drude behavior of the dynamical conductivity (Fig. 17). Second, the generalizing of this idea to interacting electrons[33] is reflected in long-time anomalies of the dynamical conductivity (Fig. 15) and a strong softening of the collective plasmons and overdamping near the metal-insulator transition (Figs. 12, 13, and 14). Third, a realistic model with finite extension of the wave functions perpendicular to the surface[17] has been used for the theory. This model brings out an improved density dependence of the dc conductivity (Fig. 1) and an increased metallic phase (Fig. 5). The dynamical consequences are most drastically documented in Fig. 10. Finite extension gives a strong suppression of the relaxation kernels in the high-frequency range and this should be measurable. Fourth, the influence of local-field corrections[21] on the static and dynamic conductivity has been demonstrated (Fig. 10). Because local-field corrections reduce the screening properties of the electron gas, the insulator phase is increased (Fig. 5). Fifth, a clear explanation of the decay mechanism of the current has been given. The increase of the relaxation kernel for low frequency is due to the decay of the current into plasmons and to the breakdown of dynamical screening (Fig. 9).

The theory is able to explain some old (Figs. 1, 2, 3, and 7) and some new experimental results (Figs. 6, 17, and 18). Furthermore, some quantitative predictions (Figs. 8, 12, 14, and 15) are made.

ACKNOWLEDGMENTS

One of us (A.G.) thanks Professor F. Koch for discussions, in particular, for suggesting the construction of Fig. 9. The other (W.G.) acknowledges useful discussions with Dr. F. Stern in connection with substrate bias effects. A.G. received support from Deutsche Forschungsgemeinschaft (Bonn, Germany), and from Sonderforschungsbereich 128.

[1]T. Ando, A. B. Fowler, and F. Stern, Rev. Mod. Phys. **54**, 437 (1982).
[2]P. W. Anderson, Phys. Rev. **109**, 1492 (1958).
[3]N. F. Mott, Electron. Power **19**, 321 (1973).
[4]A. Hartstein, T. H. Ning, and A. B. Fowler, Surf. Sci. **58**, 178 (1976).
[5]A. Hartstein, A. B. Fowler, and M. Albert, Surf. Sci. **98**, 181 (1980).
[6]N. F. Mott, M. Pepper, S. Pollit, R. H. Wallis, and C. J. Adkins, Proc. R. Soc. London Ser. A **345**, 169 (1975).
[7]S. J. Allen, D. C. Tsui, and F. de Rosa, Phys. Rev. Lett. **35**, 1359 (1975).
[8]H. R. Chang and F. Koch, Surf. Sci. **113**, 144 (1982).
[9]W. Götze, Solid State Commun. **27**, 1393 (1978).
[10]W. Götze, J. Phys. C **12**, 1279 (1979).
[11]W. Götze, Philos. Mag. B **43**, 219 (1981).
[12]A. Gold and W. Götze, J. Phys. C **14**, 4049 (1981).
[13]A. Gold, S. J. Allen, B. A. Wilson, and D. C. Tsui, Phys. Rev. B **25**, 3519 (1982).
[14]A. Gold, J. Phys. C **18**, L815 (1982).
[15]E. Abrahams, P. W. Anderson, D. C. Licciardello, and T. V. Ramakrishnan, Phys. Rev. Lett. **42**, 673 (1979).
[16]B. J. Bishop, D. C. Tsui, and R. C. Dynes, Phys. Rev. Lett. **44**, 1153 (1980); M. J. Uren, R. A. Davies, and M. Pepper, J.

Phys. C 13, L985 (1980).
[17]D. Belitz, A. Gold, and W. Götze, Z. Phys. B **44**, 273 (1981).
[18]B. L. Altshuler, A. G. Aronov, and P. A. Lee, Phys. Rev. Lett. **44**, 1288 (1980).
[19]F. Stern and W. E. Howard, Phys. Rev. **163**, 816 (1967).
[20]F. Stern, Phys. Rev. Lett. **18**, 546 (1967).
[21]M. Jonson, J. Phys. C **9**, 3059 (1976).
[22]D. Pines, P. Nozières, *The Theory of Quantum Liquids* (Benjamin, New York, 1966).
[23]R. H. Ritchie, Phys. Rev. **106**, 874 (1957).
[24]R. A. Ferrel, Phys. Rev. **111**, 1214 (1958).
[25]F. F. Fang and W. E. Howard, Phys. Rev. Lett. **16**, 797 (1966).
[26]T. Ando, J. Phys. Soc. Jpn. **43**, 1616 (1977).
[27]R. Kubo, J. Phys. Soc. Jpn. **12**, 570 (1957).
[28]R. Zwanzig, *Lectures in Theoretical Physics* (Interscience, New York, 1961), Vol. 3.
[29]H. Mori, Prog. Theor. Phys. **34**, 423 (1965).
[30]W. Götze, and P. Wölfle, Phys. Rev. B **6**, 1226 (1974).
[31]K. Kawasaki, Phys. Rev. **150**, 291 (1966).
[32]A. A. Abrikosov, L. P. Gor'kov, and I. E. Dzyaloshinski, *Methods of Quantum Field Theory in Statistical Physics* (Prentice-Hall, London, 1963).
[33]A. Gold and W. Götze, Solid State Commun. **47**, 627 (1983).
[34]D. Forster, *Hydrodynamic Fluctuations, Broken Symmetry and Correlation Functions* (Benjamin, Reading, Mass., 1975).
[35]C. Cercignani, *Theory and Application of Boltzmann Equation* (Scottish Academic, London, 1975).
[36]L. P. Kadanoff and I. Falko, Phys. Rev. **136**, A1170 (1964).
[37]J. M. Ziman, *Principles of the Theory of Solids* (Cambridge University Press, Cambridge, England, 1972).
[38]A. Gold and W. Götze, Helv. Phys. Acta **56**, 47 (1983).
[39]T. Ando, J. Phys. Soc. Jpn. **51**, 3215 (1982).
[40]P. G. de Gennes, J. Phys. Radium **23**, 630 (1962).
[41]S. Das Sharma, Phys. Rev. Lett. **50**, 211 (1983).
[42]C. Mazuré and F. Koch (unpublished).
[43]Y. Matsumoto and Y. Uemura, in Proceedings of the Second International Conference on Solid State Surfaces, Kyoto [Jpn. J. Appl. Phys. Suppl. 2, Pt. 2, 367 (1974)].
[44]N. Tzoar, P. M. Platzman, and A. Simons, Phys. Rev. Lett. **36**, 1200 (1976).
[45]N. D. Mermin, Phys. Rev. B **1**, 2362 (1970).
[46]A. Gold, W. Götze, C. Mazuré, and F. Koch, Solid State Commun. **49**, 1085 (1984).
[47]G. F. Giuliani and J. J. Quinn, Phys. Rev. B **29**, 2321 (1984).
[48]S. J. Allen, D. C. Tsui, and R. A. Logan, Phys. Rev. Lett. **38**, 980 (1977).
[49]D. Heitmann, J. P. Kotthaus, and E. G. Mohr, Solid State Commun. **44**, 715 (1982).
[50]Y. Pemeau and P. Résibois, Phys. Rep. **2C**, 63 (1975).
[51]C. Mazuré, F. Martelli, A. Gold, F. Koch, U. Grzesik, and H. R. Chang, Solid State Commun. **54**, 443 (1985).
[52]A. Gold, W. Götze, C. Mazuré, and F. Koch, in *Proceedings of the 17th International Conference on Low-Temperature Physics—LT-17, Karlsruhe, 1984* (Elsevier, Amsterdam, 1984).